PLOS PATHOGENS

RESEARCH ARTICLE

Genome-Wide fitness analysis of group B *Streptococcus* in human amniotic fluid reveals a transcription factor that controls multiple virulence traits

Allison N. Dammann[1], Anna B. Chamby[2], Andrew J. Catomeris[3], Kyle M. Davidson[4], Hervé Tettelin[5,6], Jan-Peter van Pijkeren[7], Kathyayini P. Gopalakrishna[4], Mary F. Keith[4], Jordan L. Elder[4], Adam J. Ratner[1,8], Thomas A. Hooven[4,9]*

1 Department of Pediatrics, New York University School of Medicine, New York, New York, United States of America, **2** University of Vermont Larner College of Medicine, Burlington, Vermont, United States of America, **3** Georgetown University School of Medicine, Washington, District of Columbia, United States of America, **4** Department of Pediatrics, University of Pittsburgh School of Medicine, Pittsburgh, Pennsylvania, United States of America, **5** Department of Microbiology and Immunology, University of Maryland School of Medicine, Baltimore, Maryland, United States of America, **6** Institute for Genome Sciences, University of Maryland School of Medicine, Baltimore, Maryland, United States of America, **7** Department of Food Science, University of Wisconsin, Madison, Wisconsin, United States of America, **8** Department of Microbiology, New York University, New York, New York, United States of America, **9** Richard King Mellon Institute for Pediatric Research, UPMC Children's Hospital of Pittsburgh, Pittsburgh, Pennsylvania, United States of America

* thomas.hooven@chp.edu

Citation: Dammann AN, Chamby AB, Catomeris AJ, Davidson KM, Tettelin H, van Pijkeren J-P, et al. (2021) Genome-Wide fitness analysis of group B *Streptococcus* in human amniotic fluid reveals a transcription factor that controls multiple virulence traits. PLoS Pathog 17(3): e1009116. https://doi.org/10.1371/journal.ppat.1009116

Editor: Theresa M. Koehler, University of Texas Medical School at Houston, UNITED STATES

Received: November 12, 2020

Accepted: February 18, 2021

Published: March 8, 2021

Data Availability Statement: Tn-seq reads from this study are available on the NCBI SRA server under BioProject ID PRJNA699022. RNA-seq reads are available on the NCBI GEO server under accession GSE165992.

Funding: This work was supported by NIH/NIAID (www.niaid.nih.gov) grants K08AI132555 to T.A. H., R21AI147511 to T.A.H. and A.J.R., and R01AI143290 to A.J.R.; the Pittsburgh Children's Foundation Children's Trust (www.givetochildrens.

Abstract

Streptococcus agalactiae (group B *Streptococcus*; GBS) remains a dominant cause of serious neonatal infections. One aspect of GBS that renders it particularly virulent during the perinatal period is its ability to invade the chorioamniotic membranes and persist in amniotic fluid, which is nutritionally deplete and rich in fetal immunologic factors such as antimicrobial peptides. We used next-generation sequencing of transposon-genome junctions (Tn-seq) to identify five GBS genes that promote survival in the presence of human amniotic fluid. We confirmed our Tn-seq findings using a novel CRISPR inhibition (CRISPRi) gene expression knockdown system. This analysis showed that one gene, which encodes a GntR-class transcription factor that we named MrvR, conferred a significant fitness benefit to GBS in amniotic fluid. We generated an isogenic targeted deletion of the *mrvR* gene, which had a growth defect in amniotic fluid relative to the wild type parent strain. The *mrvR* deletion strain also showed a significant biofilm defect *in vitro*. Subsequent *in vivo* studies showed that while the mutant was able to cause persistent murine vaginal colonization, pregnant mice colonized with the *mrvR* deletion strain did not develop preterm labor despite consistent GBS invasion of the uterus and the fetoplacental units. In contrast, pregnant mice colonized with wild type GBS consistently deliver prematurely. In a sepsis model the *mrvR* deletion strain showed significantly decreased lethality. In order to better understand the mechanism by which this newly identified transcription factor controls GBS virulence, we performed RNA-seq on wild type and *mrvR* deletion GBS strains, which revealed that the transcription factor affects expression of a wide range of genes across the GBS chromosome. Nucleotide biosynthesis

org/get-involved/childrens-trust) Young Investigator Award (T.A.H.); the Richard King Mellon Institute for Pediatric Research (www.chp.edu/research/rkmfi) Pilot Award (T.A.H.); and the Institute for Infection, Inflammation, and Immunity in Children Pilot Award (T.A.H.). The funders had no role in study design, data collection and analysis, decision to publish, or preparation of the manuscript.

Competing interests: The authors have declared that no competing interests exist.

and salvage pathways were highly represented among the set of differentially expressed genes, suggesting that MrvR may be involved in regulating nucleotide availability.

Author summary

Group B *Streptococcus* (GBS) is a species of Gram-positive bacteria that often colonizes the healthy adult intestinal and reproductive tracts without causing serious symptoms. During pregnancy, however, GBS can invade the pregnant uterus, where it can cause infection of the placenta, fetal membranes, and fetus—a condition known as chorioamnionitis. Chorioamnionitis is associated with serious adverse pregnancy outcomes, including stillbirth, preterm labor, and severe infection of the newborn. GBS can survive in human amniotic fluid, which is low in bacterial nutrients and contains immune molecules that limit microbial persistence, and this ability likely contributes to GBS chorioamnionitis. This study is focused on a single GBS gene that encodes a genetic regulator we called MrvR, which we show is important for GBS resistance to human amniotic fluid. Using a series of genetic techniques combined with animal models of GBS colonization and infection, we show that MrvR also plays a key role in allowing GBS to invade the bloodstream and trigger the inflammatory responses that lead to preterm labor and stillbirth. The study concludes with a survey of other GBS genes whose activity is regulated by MrvR, which seems to be an important contributor to GBS virulence.

Introduction

Streptococcus agalactiae (group B *Streptococcus*; GBS) is a cause of chorioamnionitis, stillbirth, and neonatal infections including bacteremia, pneumonia, and meningitis [1–10]. GBS is a common commensal of the intestinal and reproductive tracts in healthy adults, among whom invasive disease is rare [11,12]. In the pregnant or neonatal host, however, GBS can be highly invasive, breaching anatomic and immunologic barriers with potentially severe consequences [13,14].

GBS is known to express a number of virulence factors such as adhesins [15–17], IgA binding proteins [18–20], and the cytotoxic ornithine-rhamnopolyene β-hemolysin/cytolysin [13,21–30]. Many of these are regulated by transcription factors, some of which have been studied and described in detail [31–40], yet many of the predicted transcription factors encoded by GBS remain minimally characterized.

We have previously described development of a GBS saturated transposon mutant library and its use in Tn-seq experiments to identify essential and conditionally essential genes [41,42]. Tn-seq permits genome-wide quantification of bacterial gene fitness through highly parallel sequencing of a saturated transposon library in which transposon insertion within a given gene is expected to result in loss of that gene product [43–46]. In Tn-seq, the saturated mutant library is grown under two conditions: control outgrowth in which there is minimal selection pressure on the bacterial population (for instance, in rich media) and an experimental outgrowth condition that introduces a selective bottleneck [46]. Following DNA purification from the two conditions, next-generation sequencing is performed in a manner that allows quantification of genome-wide transposon insertion sites. By identifying transposon insertion sites that are relatively absent from the experimental outgrowth condition, it is possible to infer which genes (or potentially intergenic regions) are essential for bacterial survival

under those outgrowth circumstances [43,46–53]. Tn-seq has been widely used across a variety of bacterial species to identify genes and pathways that enable microbial survival under environmental stress [47,48,54–62]. In this study, we performed Tn-seq on GBS grown in human amniotic fluid in order to identify bacterial genes that promote survival in the nutrient-poor, unhospitable growth conditions of the amniotic sac.

The top candidate genes from our Tn-seq screen were further studied using a newly developed CRISPR interference (CRISPRi) system. Whereas wild type components of the CRISPR--Cas family of bacterial immune molecules can be used for RNA-guided, programmable double stranded DNA cleavage [63,64], two targeted mutations of Cas9 endonuclease active sites result in a catalytically inactive isoform (dCas9). Rather than introducing double stranded breaks in DNA at the site of guide RNA recognition, dCas9 can be programmed to occupy a particular region of DNA, creating steric hindrance that disrupts transcriptional initiation or elongation [65,66]. This approach allows rapid, flexible generation of functional gene expression knockdowns that permit preliminary study of a gene's phenotypic contribution without requiring generation of a targeted chromosomal deletion.

Our CRISPRi system builds on similar approaches that have been developed for other bacteria [65–69], using a plasmid-based single guide RNA (sgRNA) expression system delivered to a GBS strain in which the native *cas9* gene has been altered to render it catalytically inactive. As with CRISPRi approaches based on the canonical Cas9 enzyme from *Streptococcus pyogenes*, CRISPRi in GBS requires existence of a 20-bp DNA region complementary to the sgRNA sequence and followed by a protospacer adjacent motif (PAM) with a NGG sequence, which is the same in GBS as in *S. pyogenes* [70].

For each of the five genes found by Tn-seq to be conditionally essential for GBS survival in amniotic fluid, we identified two sgRNA sequences that met the requirements for dCas9 targeting. We then used these sequences, cloned into a sgRNA expression plasmid, to generate a pair of knockdown strains for each candidate gene. We screened these CRISPRi knockdown strains for survival defects in amniotic fluid, which allowed one form of validation of our Tn-seq data. There is evidence that the Cas9 enzyme has regulatory properties beyond its role as a bacterial immune defender against bacteriophages, and that—in GBS—some Cas9-regulated genes affect virulence [71,72]. For this reason, results of CRISPRi knockdown experiments must be viewed as provisional evidence for a particular gene's role in the bacterial phenotype, requiring further validation with a targeted gene deletion approach.

Our CRISPRi assessment of candidate genes suggested a significant survival advantage in amniotic fluid mediated by a transcription factor with domain features marking it as a member of the GntR protein superfamily. GntR regulators have a conserved helix-turn-helix DNA binding motif at the N-terminus but vary in the structure of the C-terminal effector-binding domain [73]. Based on shared similarities within the effector-binding domain, the GntR superfamily is further subdivided into four main subfamilies (FadR, HutC, MocR, and YtrA). Two minor subfamilies, AraR and PlmA, have also been described, the latter expressed only in cyanobacteria [73–77]. Conformational changes induced by ligand binding to the C-terminus of a GntR regulator alters the configuration of the N-terminus, modulating the protein's DNA binding affinity [75,77,78]. As a result of the diversity of C-terminus structures within the GntR superfamily, these transcription factors respond to a wide variety of effector ligands. Most experimentally proven GntR effectors are small molecules that are generated or consumed by central metabolic pathways [73,75,77].

We named the GBS GntR-class transcription factor with a suspected fitness role in amniotic fluid MrvR (multiple regulator of virulence). This report offers results of our whole genome Tn-seq screen, CRISPRi knockdown studies, and experiments performed with an allelic exchange gene deletion mutant strain (and an appropriate complement control strain) to

provide an initial description of the role of MrvR in several GBS virulence-related phenotypes, including survival in human amniotic fluid, *in vitro* biofilm formation, and invasive bacteremia and preterm labor in murine models. We also report transcriptomic data from RNA-seq performed with wild type GBS and a mutant strain lacking the *mrvR* gene. The transcriptomic results suggest a role in modifying expression of genes integral to nucleotide metabolism.

Results

Five GBS genes are conditionally essential for GBS survival in human amniotic fluid

Using a previously described *Himar1* transposon mutant library in an A909 (serotype Ia) background [41], we performed Tn-seq after growth challenge in eight human amniotic fluid samples from amniocentesis.

The A909 library was originally created using a temperature sensitive shuttle plasmid-based system for delivery of the *Himar1* mini-transposon and a transposase-encoding gene to electrocompetent GBS. Prior to its use in GBS, the terminal ends of the mini-transposon were modified so that they contained MmeI restriction sites. MmeI is an unusual type II restriction enzyme that cuts 20 bp downstream from its recognition site [79]. The separation between the recognition and cut sites has been exploited in Tn-seq studies, since it permits retention of transposon-adjacent host genomic DNA sequence information following MmeI digestion of transposon library DNA [45,58,80,81]. This segment of host DNA provides enough sequence specificity to pinpoint the site of transposon insertion in the source cell, which is fundamental to the Tn-seq approach.

Initial development, testing, and preliminary Tn-seq studies using our A909 library were described in detail in a prior publication [41]. Our approach to creating and characterizing the library was guided by similar work performed in *S. pyogenes* and *Streptococcus pneumoniae* backgrounds by Le Breton et al., van Opijnen, and Camilli [44,80,81]. When creating the A909 Tn-seq system, we originally produced three separate libraries, each with 36,000–100,000 unique transposon insertions. As in our prior work using Tn-seq to identify conditionally essential GBS genes in human blood [42], for this study we used a pooled mixture of the three separate libraries shown previously to have 167,000 unique mutations, which corresponds to 45% saturation of available TA-dinucleotides sites available to the *Himar1* mini-transposon in A909 [41].

Before inoculation with the GBS transposon library, the amniotic fluid used for outgrowth was filter sterilized to remove any contaminating microorganisms and human cells that may have been present. In pilot experiments with wild type A909 maintained in human amniotic fluid, we observed that an initial inoculation density of 10^8 CFU/mL decreased to 10^7 CFU/mL after overnight incubation. This decrease in CFU density suggested to us that overnight incubation in amniotic fluid exerted selective pressure against GBS without creating a severe bottleneck that would prohibit accurate calculation of gene contributions to fitness. We therefore used an overnight incubation strategy in our Tn-seq library selection experiment.

The eight amniotic fluid samples used for outgrowth were comprised of two or three equal-volume aliquots from three separate women. The purpose of this design was to ensure that neither donor-specific (such as antibiotic exposure or chorioamnionitis at the time of amniocentesis) nor sample-specific (microbial contamination, for instance) factors influenced the Tn-seq outcome. Each amniotic fluid aliquot was seeded independently with the A909 transposon library. The same pooled mutant library was grown in rich media as an input control. Following 16-hour experimental or control incubation and a subsequent outgrowth phase in rich media to increase biomass, DNA was purified from each sample and processed for Tn-seq by

MmeI digestion and subsequent ligation of separate, barcoded double-stranded DNA adapters to the resultant DNA sticky ends. The final step was PCR amplification of transposon-genome junctions, followed by next-generation sequencing of the resulting amplicon library.

We used ESSENTIALS, a publicly available Tn-seq bioinformatics package, to analyze sequencing data from the Tn-seq experiment [50]. ESSENTIALS takes sequencing reads or alignment files as input; in this instance, we performed initial alignment of our Tn-seq data to the A909 genome using Bowtie 2 [82]. Following data upload, ESSENTIALS normalizes read counts across control and experimental replicates using the trimmed mean of M values (TMM), which corrects for differential sequencing depth and potential compositional biases resulting from experimental depletion of the mutant library [83]. Following normalization, statistical differences in gene transposon insertion are determined using an exact test performed within the negative binomial distribution statistical model in EdgeR [84]. Following this statistical testing, each nonessential gene's contribution to fitness can be assessed by the $\log_2$ transformed ratio of transposon insertions detected in the experimental condition relative to control. This ranked list, with associated p values from the exact test, is a useful way to compare relative fitness contributions (**S1 Data**). However, ESSENTIALS also generates a kernel density plot of experimental-versus-control insertions and calculates local minima on that plot (**S1 Data, bottom**), which can provide a more stringent separation of conditionally essential genes from those with less of a contribution to fitness [50]. We used this local minimum calculation to identify five candidate conditionally essential genes expected to have the most significant contribution to GBS survival in amniotic fluid (**Fig 1 and Table 1**).

One of the candidate genes, SAK_RS10120, which we termed *mrvR*, had conserved functional domains suggesting its membership in the GntR superfamily of transcriptional regulators. The other candidate genes encoded an expected DeoR family transcriptional regulator (SAK_RS09545), a predicted membrane-spanning protein of unknown function (SAK_RS05160), an ABC-class transporter (SAK_RS09890), and one protein (SAK_RS02930) with a single domain of unknown function whose cellular localization and role are also unknown.

CRISPRi knockdown and targeted knockout competition assays validate Tn-seq findings

To further validate the five candidate genes conditionally essential for GBS survival in amniotic fluid, we developed a CRISPRi gene expression knockdown system, which uses natively expressed, catalytically inactive Cas9 (dCas9) encoded on the GBS chromosome along with a single guide RNA (sgRNA) expression plasmid to generate efficient and flexible gene expression inhibition in GBS. We competed knockdowns of the five candidate conditionally essential genes against a sham targeting control dCas9 strain in human amniotic fluid and assayed survival using quantitative PCR analysis of knockdown and control strain persistence.

Development of a GBS CRISPRi system was aided by the fact that the GBS *cas9* gene shows high sequence similarity to the canonical *cas9* endonuclease first described in *S. pyogenes* [64,85–87] (**S1 Fig**). This homology allowed us to predict the two missense mutations that would establish a catalytically inactive isoform in GBS: D10A and H840A. Lopez-Sanchez et al. have previously shown that the protospacer adjacent motif (PAM) necessary for GBS Cas9 genomic target recognition follows the same NGG pattern as in *S. pyogenes* [70]. We used a previously described sucrose-counterselectable mutagenesis plasmid, pMBsacB, to generate point mutations within the coding sequence of the *cas9* gene in GBS strain CNCTC 10/84 (serotype V) [88], which is the strain with which our animal models of vaginal colonization and ascending chorioamnionitis have been optimized.

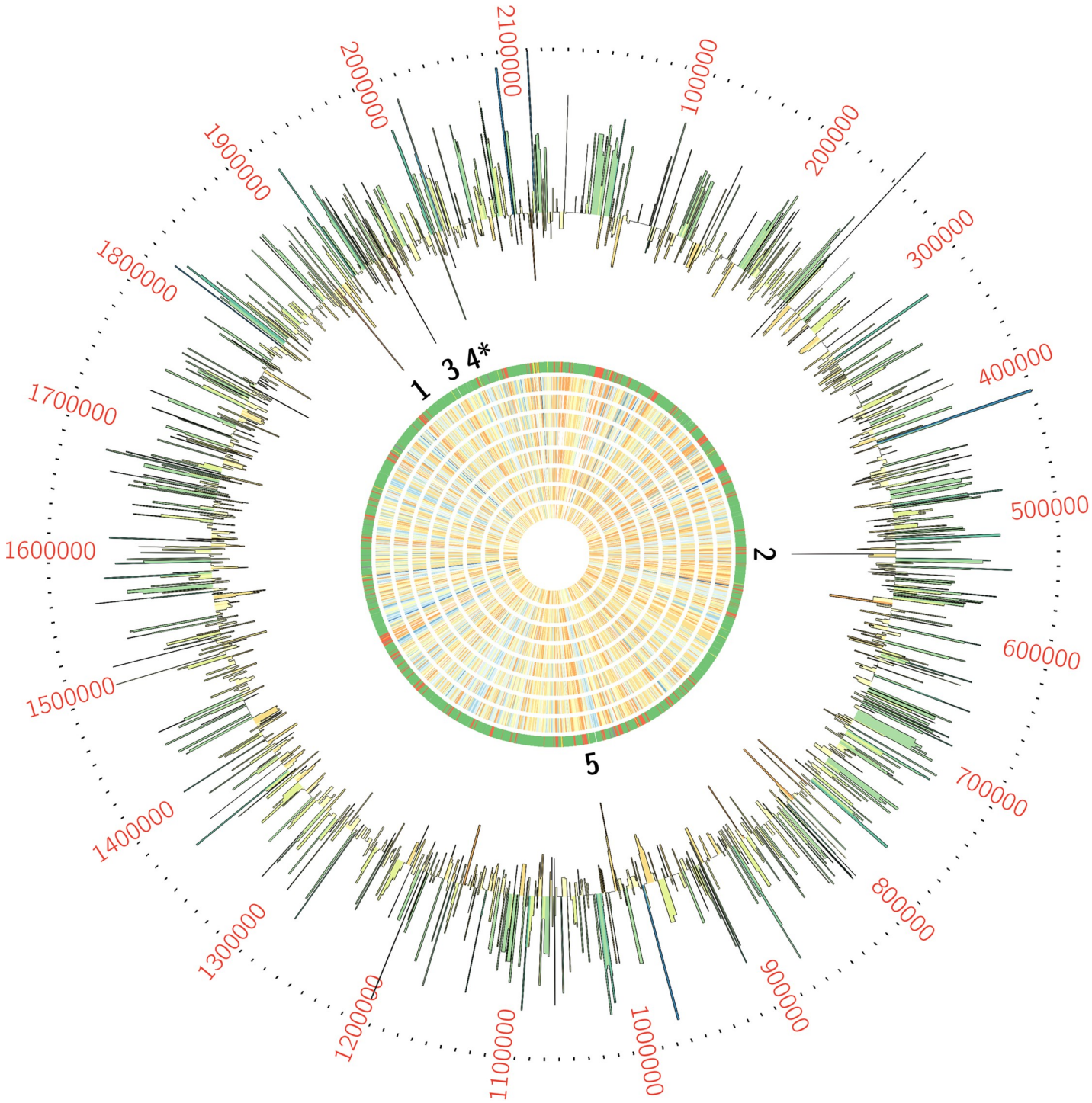

Fig 1. Tn-seq screening of GBS grown in human amniotic fluid revealed 5 conditionally essential genes. GBS transposon library in a background of strain A909 was grown in eight human amniotic fluid samples from three individuals (see main text), then subjected to Tn-seq analysis. Each ring of the Circos plot shows a different representation of the A909 circular chromosome. From the center of the plot, rings 1–8 show transposon insertion density detected in the eight amniotic fluid outgrowth samples (lowest detection: red; highest detection: blue). Ring 9 shows essential genes (red), nonessential genes (green), intermediate genes (yellow), and those for which baseline fitness cannot be determined (white; see reference [41]). The outermost ring shows $\log_2$ fold-change values for each gene in amniotic fluid outgrowth as determined by ESSENTIALS. Genes with inward-pointing peaks had fewer than expected transposon insertions. Outward-pointing peaks had more than expected transposon insertions. The peaks are color coded for statistical significance (low adjusted p value: red; high adjusted p value: green). The five labeled peaks are described in the text and are listed in **Table 1**. Peak 4 is the GntR-class transcription factor, *mrvR*.

https://doi.org/10.1371/journal.ppat.1009116.g001

Table 1. GBS genes conditionally essential for survival in human amniotic fluid.

Gene locus	log_2 Fold-Change[a]	Expected product
SAK_RS09545	-4.3690439	DeoR family transcriptional regulator
SAK_RS02930	-4.3341605	hypothetical protein
SAK_RS09890	-4.1865043	ABC-class transporter
SAK_RS10120	-3.8123495	GntR family transcriptional regulator (mrvR)
SAK_RS05160	-3.7270772	membrane-spanning protein of unknown function

a Fold-change between expected and observed transposon insertions in amniotic fluid experimental outgrowth conditions

https://doi.org/10.1371/journal.ppat.1009116.t001

We developed a sgRNA expression shuttle plasmid, p3015b, which accepts ligation of a 20-bp protospacer against a target gene between two BsaI restriction enzyme recognition sites. We used the Broad Institute's Genetic Perturbation Platform sgRNA design tool (https://portals.broadinstitute.org/gpp/public/analysis-tools/sgrna-design) to select optimized protospacers [89,90]. After confirming successful protospacer cloning in an *E. coli* background, the targeting plasmids were purified and transformed into competent 10/84 modified to express dCas9.

To establish proof-of-concept for this approach we knocked down the first open reading frame (*cylX*) in the *cyl* operon that encodes genes responsible for synthesis of the pigmented cytotoxin β-hemolysin/cytolysin [91]. p3015b encoding anti-*cylX* sgRNA could not be transformed into wild type GBS, presumably because Cas9 targeting to the chromosome resulted in lethal double-stranded DNA cleavage. The dCas9 strain, however, had high transformation efficiency and generated non-pigmented, non-hemolytic knockdowns when transformed with plasmid expressing anti-*cylX* sgRNA (**Fig 2A**).

Next, we created plasmids targeting two different sites in each of the five candidate amniotic fluid conditionally essential genes (**Fig 2B**) and transformed dCas9-expressing 10/84. The Broad Institute's Genetic Perturbation Platform allows prioritization of sgRNA-complementary target sites with certain characteristics [89,90]. Where possible, we selected targets in the first half of the candidate gene coding sequence, without polynucleotide repeats greater than four bases, and without overlap of the two target sequences. These criteria were met for three of the five candidate genes, but were not universally achievable: overlap of the two target sequences was required for the *deoR* gene and one of the two hypothetical protein targets was in the second half of the coding sequence.

The resulting knockdown strains, plus a control dCas9 strain transformed with p3015b bearing a sham protospacer, were tested through qRT-PCR for target gene silencing. After growth to stationary phase, reverse transcribed cDNA from each knockdown and the non-targeted control was normalized to *recA*, a stably expressed GBS housekeeping gene [92]. For each knockdown strain, the targeted gene's normalized expression was compared to the non-targeting control strain using gene-specific PCR primers (**S1 Table**). This analysis showed significant silencing of the target genes in eight of the ten knockdown strains (**S2 Fig**). The ABC transporter gene did not show significant silencing at stationary phase by qRT-PCR. We did not rule out the possibility that off-target amplification of another chromosomal region accounted for this apparent escape from silencing.

In order to use our knockdown strains for initial validation of our Tn-seq results, they were combined and used to inoculate erythromycin-selective amniotic fluid (one of the three samples that was used for Tn-seq) and control broth. At the time of inoculation (T_0), an aliquot of each combined sample was used for plasmid DNA extraction. After 24 hours of competition

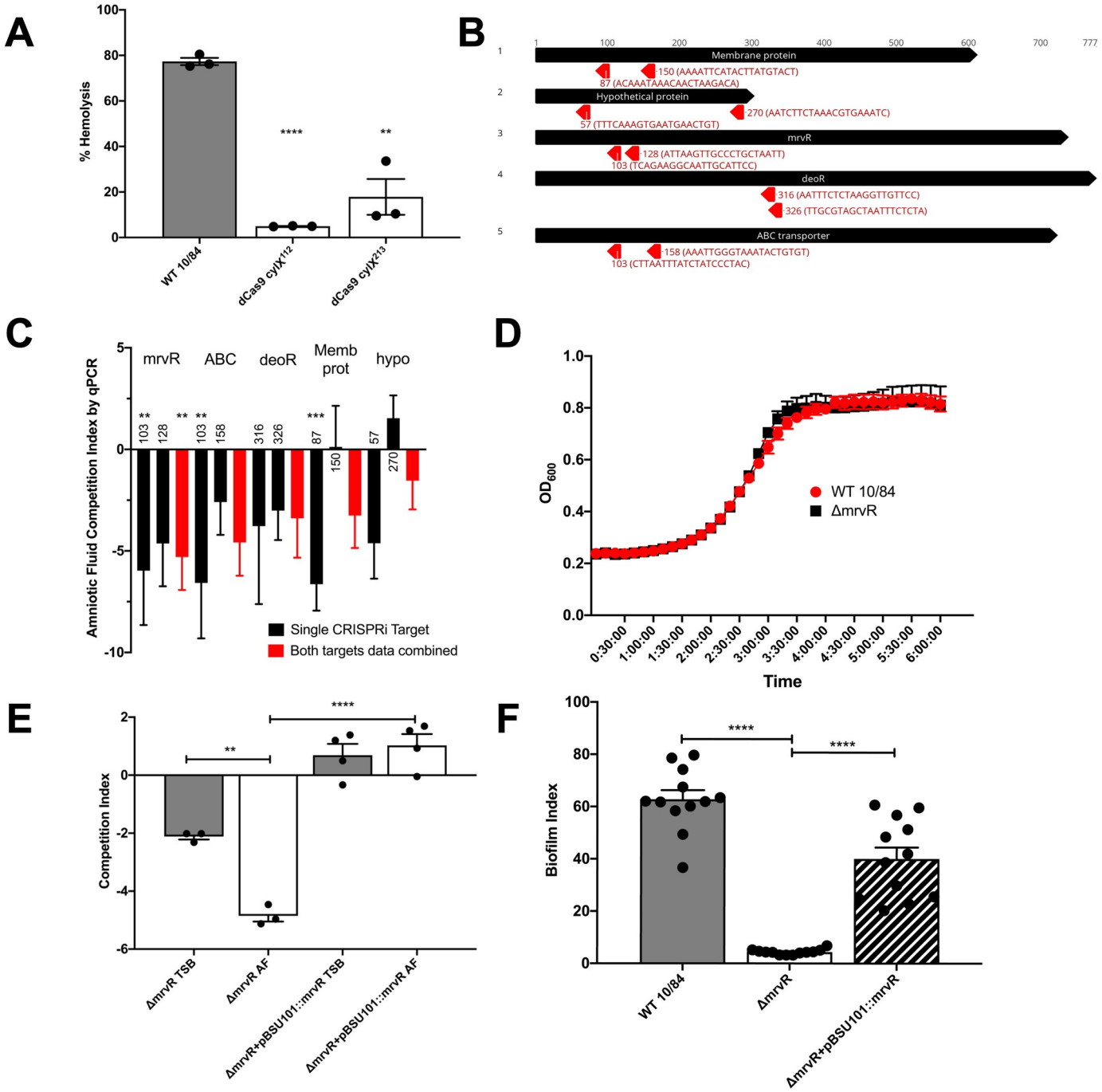

Fig 2. CRISPRi knockdowns of candidate genes and phenotypic characterization of GBS lacking MrvR in amniotic fluid, rich media, and biofilm-promoting growth conditions. Two CRISPRi targeting protospacers (targeting nucleotides 112 and 213 of *cylx*, the first gene in the operon) against the *cyl* operon were developed to knockdown expression of β-hemolysin/cytolysin. The resultant knockdown strains (in a 10/84 background) were compared to wild type in a human erythrocyte hemolysis assay (**A**). Targeting protospacers against the five candidate conditionally essential genes from amniotic fluid Tn-seq. For each gene, the number indicates the targeted nucleotide; the protospacer sequence is shown in parentheses (**B**). A qPCR-based multiplex CRISPRi screen using knockdowns of all five candidate genes revealed decreased fitness in amniotic fluid compared to tryptic soy (TS) broth (**C**); black columns show the competition index of strains bearing individual targeting protospacer plasmids, while red columns show pooled results from both targeting plasmids for each gene. Statistical significance of each knockdown phenotype was determined relative to growth of the knockdowns in TS broth. Growth curves of the Δ*mrvR* and wild type (WT) 10/84 in broth (**D**). Colony forming unit enumeration-based competition assays between Δ*mrvR* and Δ*mrvR*+pBSU101::*mrvR* in TS broth (TSB) and amniotic fluid (AF); **E**). Biofilm assay results comparing WT 10/84, Δ*mrvR*, and Δ*mrvR*+pBSU101::*mrvR*. (* $p<0.05$, ** $p<0.01$, *** $p<0.005$, **** $p<0.001$; t test, error bars show standard error surrounding mean).

https://doi.org/10.1371/journal.ppat.1009116.g002

(T_{24}), plasmid DNA was purified from each broth and amniotic fluid sample. We used protospacer-specific quantitative PCR primers to characterize T_0 and T_{24} GBS as a CRISPRi knockdown or non-targeting control. We used the qPCR results to calculate competition indices for the knockdowns, then compared competition indices in amniotic fluid to broth. The experimental design is diagrammed in S3 Fig. Fig 2C shows the results from two replicates of this experiment and demonstrates an expected competition defect in amniotic fluid for the five candidate knockdown strains.

A targeted knockout of mrvR shows a growth defect in human amniotic fluid

MrvR showed a consistent CRISPRi knockdown pattern, where both targeting protospacers generated a fitness defect in amniotic fluid. We selected this gene for further study based on these results and the hypothesis that this transcription factor may bridge microenvironmental changes associated with exposure to amniotic fluid and gene expression responses that promote amniotic fluid survival and possibly other GBS virulence traits.

Using pMBsacB, we generated an isogenic knockout of W903_RS09645, the *mrvR* ortholog in 10/84. We also complemented the gene deletion by cloning the full coding sequence of W903_RS09645 and its upstream promoter sequence into the shuttle vector pBSU101 (replacing the green fluorescent protein and *cfb* promoter sequence originally cloned into pBSU101) [93] and transforming the knockout with this plasmid.

We tested the knockout and complemented strains for survival defects in human amniotic fluid and in broth. Fig 2D shows growth curves of the wild type and knockout strains in tryptic soy broth, indicating that growth kinetics between the two strains in rich media are identical. Fig 2E shows results of competition assays in which amniotic fluid and broth were inoculated with a mixture of wild type 10/84 and the knockout strain or its complement. After 24 hours of outgrowth, these mixtures were plated for CFU enumeration on selective and nonselective media, permitting determination of the relative survival of the strains in competition.

We observed that in broth the knockout strain had a mild survival defect relative to wild type—despite similar growth kinetics in monoculture conditions—but that the defect was more severe in amniotic fluid, and that both defects could be complemented through expression of the full-length *mrvR* gene.

MrvR controls GBS biofilm formation

We observed phenotypic differences in growth of the *mrvR* knockout as compared to wild type 10/84. In liquid media, the mutant seemed to aggregate in clumps with less coating of the outgrowth vessel, although there were no obvious morphologic differences when the cells were examined by light microscopy after Gram stain (S4 Fig). We suspected that the knockout was biofilm deficient, which we confirmed using a biofilm assay. The biofilm index is the ratio of crystal-violet stained biofilm (following overnight growth in a multi-well plate) divided by the planktonic-phase optical density from the same sample. Fig 2F confirms that the knockout mutant is biofilm deficient compared to wild type 10/84, and that the biofilm phenotype is restored in the complemented strain.

MrvR activity does not affect vaginal colonization

To test whether *mrvR* is necessary for persistent vaginal colonization, we colonized healthy adult female mice with knockout GBS or wild type control and performed serial surveillance swabs using an established protocol [13]. After estrus synchronization with β-estradiol administration, nonpregnant adult C57BL/6J mice were colonized with equal inoculums of

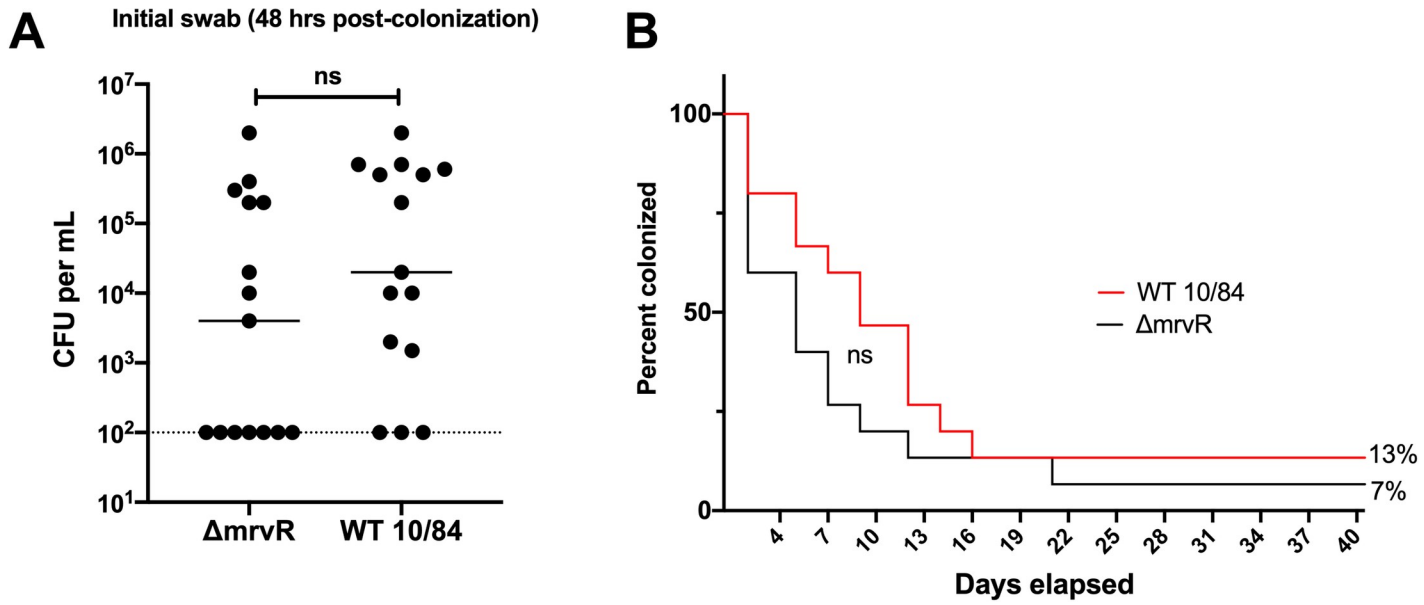

Fig 3. MrvR does not affect establishment or maintenance of vaginal colonization. Adult nonpregnant C57/BLJ mice were vaginally colonized with wild type (WT) 10/84 or Δ*mrvR*. Neither the colonization density at the initial swab 48 hours after inoculation (**A**; t test) nor duration of colonization (**B**; Mantel-Cox test) showed significant differences (CFU: colony forming units, ns: not significant).

https://doi.org/10.1371/journal.ppat.1009116.g003

stationary-phase wild type 10/84 or *mrvR* knockout GBS. Following colonization, the mice were single-housed and screened for colonization persistence three times weekly (starting 48 hours after colonization) by plating vaginal swab samples on GBS-specific chromogenic agar. We did not include the complemented knockout in this experiment because of past observations that, without ongoing *in vivo* antibiotic selection, plasmid DNA is rapidly cured by colonizing GBS.

While there was a trend toward earlier clearance among the mice colonized with the mutant strain, neither initial colonization density nor eventual clearance among the two groups differed significantly (Fig 3).

The MrvR knockout causes chorioamnionitis without preterm delivery in a mouse model

To test the effect of *mrvR* in ascending chorioamnionitis, we used an established mouse model, vaginally colonizing pregnant female mice on pregnancy day 13 with either wild type 10/84 or the *mrvR* knockout.

Colonized pregnant mice were monitored through pregnancy day 17. Preterm delivery between day 13 and day 17 by a colonized mouse was one experimental endpoint, while animals that remained pregnant on day 17 were sacrificed and assessed for persistent vaginal colonization and ascending chorioamnionitis. Chorioamnionitis was established based on any of the following: GBS present in placental homogenates, GBS present in fetal homogenates, or GBS present in amniotic fluid. Data from mice that were no longer vaginally colonized on day 17 were not included in the analysis; none of the mice who cleared their vaginal colonization had chorioamnionitis.

There was a significant difference between pregnancy outcomes for mice colonized with wild type GBS and those colonized with the knockout. Whereas eight of eleven mice colonized with wild type GBS delivered preterm, none of the eleven mice colonized with the knockout

strain did. However, all of the knockout colonized mice had chorioamnionitis with widespread GBS dissemination throughout the placentas, fetuses, and amniotic fluid. Of the mice colonized with wild type GBS, two of the three that carried their pregnancies through day 17 had chorioamnionitis (**Fig 4A and 4B**).

Colony counts from tissue and amniotic fluid samples collected at laparotomy showed a significant difference between wild type and knockout GBS density in amniotic fluid but not placental or fetal tissue. Bacterial density was higher in placental homogenates than in fetal tissue homogenates and amniotic fluid for both GBS strains, suggesting the placenta as the portal of infection (**Fig 4C**).

MrvR is necessary for lethal invasive bacteremia in a murine sepsis model

To assess the role of the transcription factor in bloodstream invasion and systemic infection, we performed intraperitoneal injections of knockout and wild type GBS in healthy adult BALB-c mice. Both bacterial strains were transformed with a toxin-antitoxin stabilized plasmid expression system that generates constitutive luciferase, permitting *in vivo* monitoring of bacterial spread upon bacterial exposure to luciferin cofactor.

The infected mice were photographed using an IVIS *in vivo* imaging system at the time of initial intraperitoneal infection, then daily afterward until either death or complete clearance of the luciferase signal. Surviving mice that had cleared their infection based on imaging were subsequently observed for the following five days, and all remained well-appearing with normal behavior, eating, and stable weights throughout this post-imaging observation period.

This experiment revealed a significant difference in the ability of infected mice to clear mutant and wild type GBS. Whereas 87% of mice infected with wild type GBS died of the infection within three days, none of the mice infected with the knockout strain died. *In vivo* imaging showed that the mice were able to contain and clear the knockout strain, while the wild type strain tended to invade beyond the peritoneum such as into the thorax, a finding that was invariably followed by death (**Fig 5**).

Whole-genome transcriptomics shows that MrvR affects a widespread genetic network including multiple operons involved in nucleotide metabolism

We performed whole-genome RNA-seq on wild type GBS and the *mrvR* knockout in order to gain a preliminary understanding of the transcription factor's regulon. We purified RNA from liquid cultures of the two strains at three growth time points: early log phase, late log phase, and stationary phase.

Comparing gene expression between the knockout and wild type GBS demonstrated that a substantial fraction of GBS transcription is controlled directly or indirectly by MrvR (**Fig 6A and S2 Data**). 16.8 percent of genes showed at least a 2-fold change in expression in the knockout relative to wild type during early logarithmic growth. This total increased to 35.7 percent in late logarithmic phase before dropping to 19.9 percent in stationary phase. A principal component analysis of the RNA-seq data showed clustering of the two knockout late log samples apart from both strains in early log phase and stationary phase (**Fig 6B**), reinforcing the concept that MrvR exerts its major regulatory influence during the transition from late log to stationary growth. A correlation analysis using sequence counts across the entire genome showed reproducibility between technical replicates and also that the knockout late log expression profile occupied its own clade on hierarchical clustering (**S5A Fig**). Heatmaps of the top 500 differentially expressed genes (**S5B Fig**) demonstrate distinct but reproducible profiles across conditions.

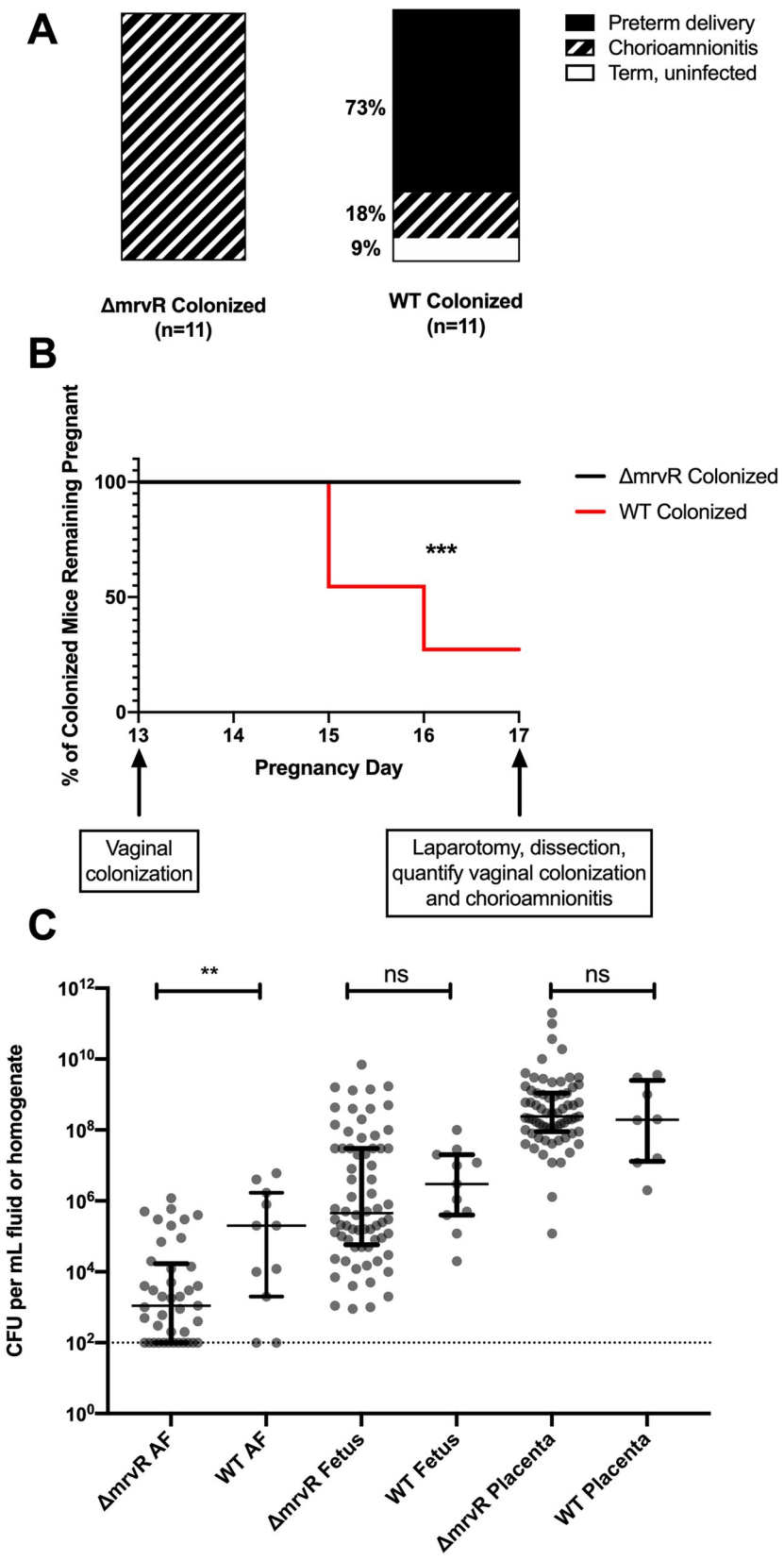
A
Preterm delivery
Chorioamnionitis
Term, uninfected
73%
18%
9%
ΔmrvR Colonized
(n=11)
WT Colonized
(n=11)
B
% of Colonized Mice Remaining Pregnant
100
50
0
***
13
14
15
16
17
Pregnancy Day
ΔmrvR Colonized
WT Colonized
Vaginal colonization
Laparotomy, dissection, quantify vaginal colonization and chorioamnionitis
C
CFU per mL fluid or homogenate
10^{12}
10^{10}
10^{8}
10^{6}
10^{4}
10^{2}
10^{0}
**
ns
ns
ΔmrvR AF
WT AF
ΔmrvR Fetus
WT Fetus
ΔmrvR Placenta
WT Placenta

Fig 4. MrvR has a significant effect on the outcome of chorioamnionitis. Pregnant BALB/c mice were vaginally colonized with wild type (WT) or knockout (KO) 10/84 on pregnancy day 13. Pregnancies were monitored until day 17 or preterm delivery, whichever came first. On day 17, mice that remained pregnant were dissected and evaluated for vaginal colonization and chorioamnionitis. While none of the KO-colonized mice with chorioamnionitis delivered preterm, 8 of 11 WT-colonized mice delivered early. One WT-colonized mouse did not develop chorioamnionitis (**A-B**; *** $p<0.005$; Mantel-Cox test). Dissected pregnancy tissue was homogenized and quantified, showing a difference in invasion density in amniotic fluid (AF) but not in fetal or placental tissue (**C**, ** $p<0.01$; t test, error bars show interquartile ranges surrounding medians; ns: not significant).

https://doi.org/10.1371/journal.ppat.1009116.g004

Notably, a prophage island from W903_RS03075 through W903_RS03520 showed significant downregulation in the knockout at all three phases of growth. In order to confirm that this prophage DNA remained present in the knockout and had not undergone excision, we performed PCR amplification of three prophage regions using genomic DNA template from the wild type and mutant GBS strains (**S6A and S6B Fig**). We also used qRT-PCR on cDNA from separate cultures to validate our RNA-seq data that showed decreased expression of genes within the prophage island in the mutant (**S6C Fig**).

We used a publicly available gene set enrichment search tool [94] to assess the differential gene expression data for functional patterns. This analysis revealed that genes involved in purine and pyrimidine metabolism were significantly enriched among the set of differentially expressed genes and that these nucleotide metabolism genes showed differential expression across all three growth phases. Other functional categories that showed significant differential expression tended to only be affected in one or, at most, two phases of growth (**Fig 6C–6G**).

The *mrvR* gene is located next to a uridine phosphorylase gene (W903_RS09640), which encodes the Udp enzyme that converts uridine to uracil. The intergenic region between *mrvR* and *udp* is 158 nt. The *udp* gene appears coregulated by MrvR, based on RNA-seq data indicating significant upregulation of *udp* expression in the knockout strain relative to wild type. Intriguingly, the arrangement of MrvR adjacent to nucleotide metabolic genes—particularly uridine phosphorylase genes—is highly conserved across Gram-positive bacteria (**S7 Fig**).

Discussion

GBS can survive and grow in diverse environments within the human host. It can persist in the intestine, in the male and female reproductive tracts, within the placenta, the amniotic fluid, human blood, joint spaces, the neonatal lung, and the central nervous system [1,9,12,33,95–99]. This environmental tolerance contributes to GBS virulence, allowing it to invade and grow within compartments that are prohibitive to other bacteria.

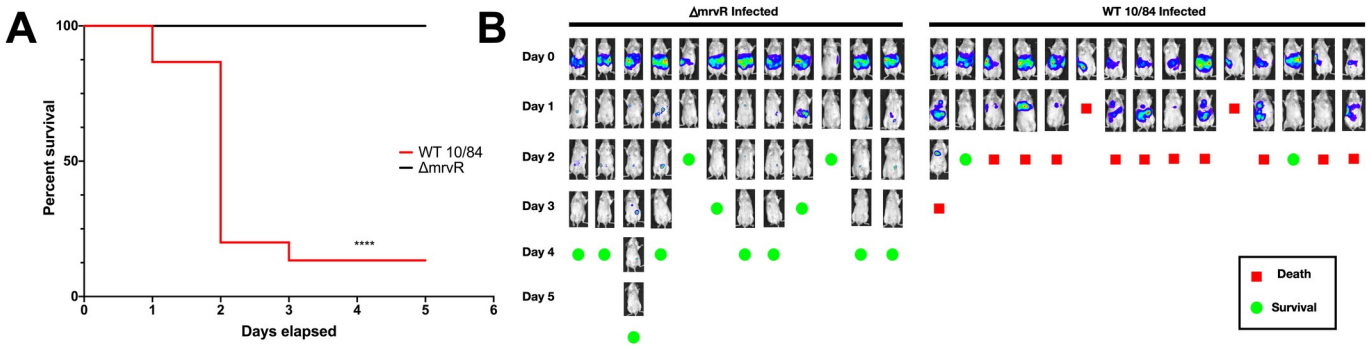

Fig 5. MrvR affects GBS invasiveness and lethality in a sepsis model. BALB/c mice were infected intraperitoneally with wild type (WT) 10/84 or Δ*mrvR*, both bearing a plasmid to allow *in vivo* tracking of a luciferase signal. There was a significant difference in outcome between the two strains (**A**, **** $p<0.001$ Mantel-Cox test). Mice were imaged daily (**B**) until they either died (red boxes) or completely cleared the luciferase signal (green circles). Mice that cleared the luciferase signal were monitored for the following five days and remained well.

https://doi.org/10.1371/journal.ppat.1009116.g005

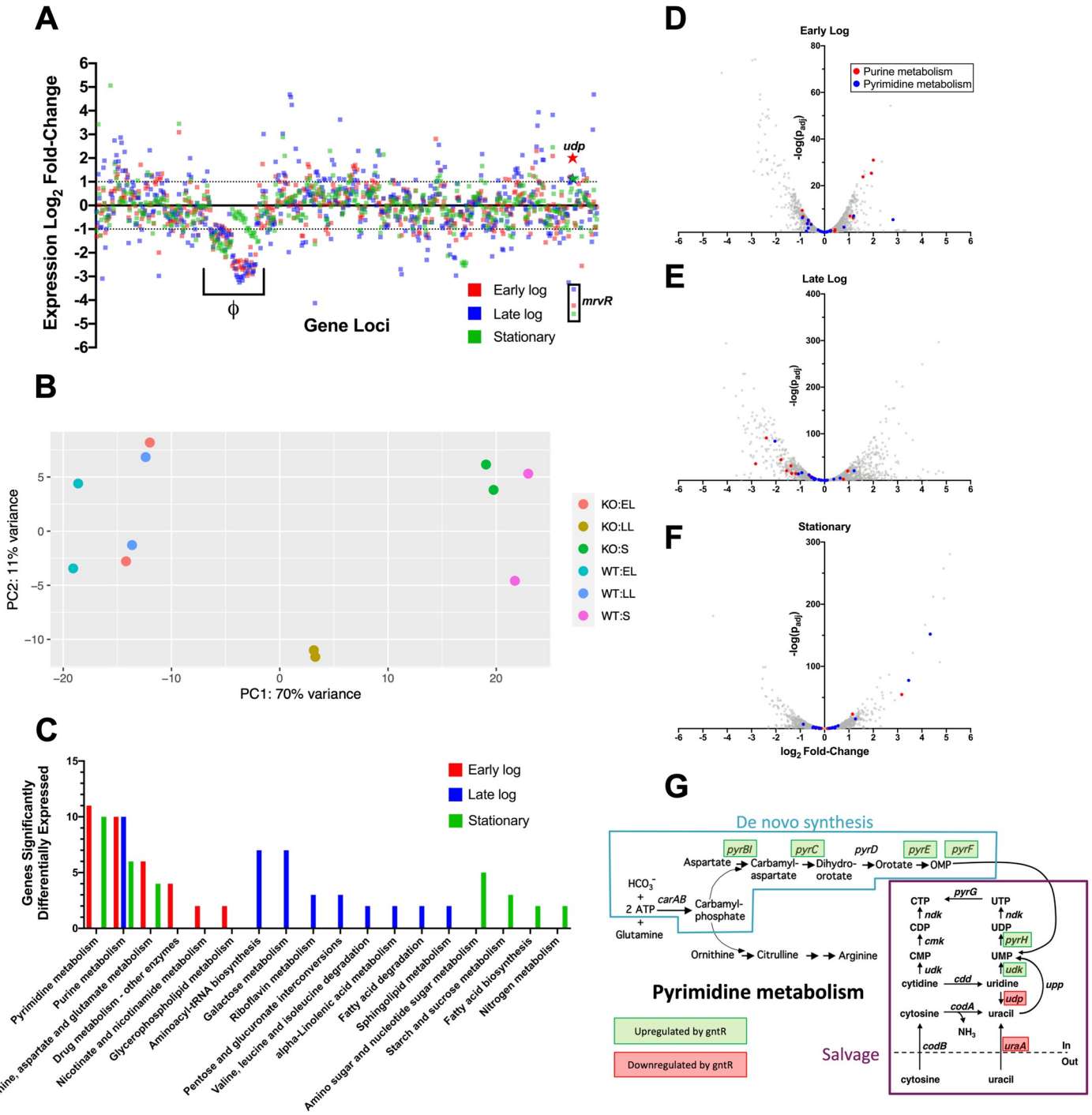

Fig 6. Analysis of the MrvR regulon reveals widespread effects with emphasis on genes involved in nucleotide metabolism. RNA-seq analysis of wild type (WT) and Δ*mrvR* 10/84 at three growth timepoints showed extensive regulation across the chromosome in all phases of growth (**A**, expression $\log_2$ fold-change shown relative to WT). A phage island (Φ) with significant differences from WT is noted, as are the *udp* gene (stars) and *mrvR*, which was deleted in the knockout strain. Principal component analysis showed isolated clustering of the late log phase replicates of the knockout strain (**B**). Gene set enrichment analysis showed that, across all three bacterial growth phases tested, the KEGG pathways most influenced by the presence of MrvR were pyrimidine and purine metabolism (**C**), which is also shown in volcano plots (**D-F**). Panel **G** shows specific genes of the de novo and salvage pathways of pyrimidine metabolism in GBS whose expression is significantly affected by the presence of MrvR (KO = Δ*mrvR* knockout; EL = early log; LL = late log; S = stationary).

https://doi.org/10.1371/journal.ppat.1009116.g006

This study began with a Tn-seq examination of genes that promote GBS fitness in amniotic fluid. GBS survival within human amniotic fluid contributes to its ability to cause ascending chorioamnionitis, which can lead to preterm labor and early-onset sepsis, sometimes in combination—a circumstance that can result in delivery of a severely infected preterm newborn with multi-organ system dysfunction [14,100–103]. Intraamniotic infection can also result in stillbirth [10]. Amniotic fluid has chemical and immunological characteristics that are antimicrobial. The fetus and membranes produce antimicrobial peptides that inhibit bacterial survival, and amniotic fluid is intrinsically poor in nutrients required for bacterial proliferation [104–112].

We identified five GBS genes required for survival in human amniotic fluid. Two of these were predicted to encode transcriptional regulators, two encode surface-associated proteins, and one remains uncharacterized. A previous study that used a proteomic approach to evaluate differential gene expression in GBS strain A909 (the same background used for our Tn-seq library) during conditions associated with colonization and fetal invasion did not identify any of the same genes [113]. Intriguingly, however, that investigation found two differentially expressed proteins (encoded by SAK_RS10135 and SAK_RS09535) whose genes are both two loci away from members of our set.

Our analysis also suggests that a significant set of gene deletions increase GBS fitness in amniotic fluid. We speculate that, when GBS enters the stringent conditions of human amniotic fluid, nonessential accessory gene expression may carry a high cost due to the limited metabolic resources available. If this is the case, removal of genetic pathways that expend energy without enhancing immune defense or required biosynthetic capacity may promote enhanced survival.

This study introduces a novel CRISPRi gene expression knockdown system, which we paired with qPCR to further interrogate the candidates suggested by our Tn-seq screen (65, 68, 69).

Our GBS CRISPRi system—which permits flexible and rapid phenotypic discovery without the challenge and time requirements associated with generating gene deletions on the chromosome—could be used for diverse experimental purposes. In this case, it allowed us to validate Tn-seq results and to decide which candidate gene to further study. We envision additional uses, however, including rapid generation of knockdown libraries for multiplex testing of gene contributions to fitness in GBS and exploration of the roles of essential genes whose expression cannot be eliminated entirely.

In this study, the CRISPRi screen pointed our attention to a GntR-class transcription factor that seemed to play an important role in bacterial fitness in amniotic fluid. While GntR transcription factors are widely distributed throughout the bacterial kingdom, and some have been shown to play a role in virulence [73,77,114–120], this gene's role in GBS host-pathogen interactions has not been explored. Interestingly, an orthologous gene was previously shown to influence group A *Streptococcus* susceptibility to the mouse cathelicidin CRAMP during murine skin infection [121]. We investigated whether our knockout GBS had altered CRAMP sensitivity, but did not observe an effect. Instead we focused on various GBS phenotypic features that are regulated by this transcription factor.

We confirmed our CRISPRi knockdown findings with survival assays in broth and human amniotic fluid, using an in-frame deletion of the transcription factor, which we competed against the wild type parent strain. Unexpectedly, the MrvR knockout was visibly deficient at forming biofilms, which we subsequently confirmed with formal biofilm assays. GBS biofilms have been posited to influence colonization and host immune evasion in GBS and other bacteria [16,122–124].

In a murine model of chorioamnionitis, absence of MrvR had a major impact on the ability of GBS to trigger preterm birth, with mice colonized on pregnancy day 13 showing consistent carriage of their pregnancies through day 17, despite extensive uterine invasion of the

knockout strain. This is in contrast to the high rates of preterm delivery seen when pregnant mice are vaginally colonized with wild type GBS, which was observed in this study and in prior work [13] and has been documented in other animal models and clinical practice [14,29].

This finding adds to accumulating evidence that GBS invasion of the fetoplacental unit is not, in itself, sufficient to trigger preterm delivery. A previous study demonstrated similar findings in an examination of the role of β-hemolysin/cytolysin in chorioamnionitis and preterm birth [13]. Several others have shown that consequential inflammatory cascades are triggered in the choriodecidua following GBS invasion [14,24,30,125]. We hypothesize that these inflammatory cascades are enhanced by expression of virulence factors regulated by MrvR, such that its absence ameliorates the inflammation that leads to preterm birth without preventing tissue invasion; this hypothesis will be the focus of additional future work.

Our work also shows that pathways regulated by MrvR are critical for bloodstream invasion and host immune evasion. In an adult mouse model of sepsis, dramatic differences were seen between wild type and knockout GBS in terms of systemic spread and eventual mortality.

Our transcriptomic analysis of the *mrvR* knockout suggests that this transcription factor is involved in mediating nucleotide metabolism. Purine and pyrimidine sensing, biosynthesis, and salvage all play key roles in modulation of virulence traits in other bacterial pathogens [126–128]. Furthermore, intracellular nucleotide homeostasis is highly regulated through diverse signaling pathways [126,129,130], lending plausibility to the prospect that the transcription factor under study here also participates in maintaining nucleotide concentrations.

It is interesting and potentially informative that the major virulence effects of MrvR seem to be manifest in anatomic compartments that are normally sterile (the uterus, peritoneum, and bloodstream), whereas its effects in the nonsterile vaginal colonization model were minimal or altogether absent. We speculate that the presence of a diverse microbiota in the vaginal milieu may complement whatever nucleotide biosynthetic pathway or pathways MrvR serves to modulate in the sterile environments associated with invasive disease.

We used two GBS strains for this study: A909 and CNCTC 10/84. A909 is a serotype Ia strain that was a clinical isolate originally collected by Rebecca Lancefield [131]. 10/84 is a serotype V strain, also a clinical isolate [132], with a hyperpigmented, hypervirulent phenotype observed in a subset of disease-causing GBS [25]. Both strains have been used in numerous GBS pathogenesis studies. The MrvR protein sequence is identical in the two strains except for a single phenylalanine (10/84) to leucine (A909) difference at position 191 of 245. Prior work demonstrated that the orange pigmentation and hypervirulence of 10/84 result from overexpression of the ornithine-rhamnopolyene β-hemolysin/cytolysin, which has cytotoxic properties [26,28–30,133]. Shortly before completion of the *in vivo* experiments for this study, Zhu et al. published data showing that 10/84's overexpression of β-hemolysin/cytolysin results from a single nucleotide polymorphism in the noncoding promoter region of the *covR*/*covS* two-component regulatory system, resulting in relative under-expression compared to GBS strains without this mutation [134]. The fact that *mrvR* had an effect on GBS survival in amniotic fluid in A909 and 10/84 suggests that its role in 10/84 is not due to the altered *covR*/*covS* expression, but future work will be applied toward determining the role of *mrvR* across multiple GBS strains, as well as seeking to better understand its exact molecular mechanism, including its DNA binding sites and effector molecule.

In conclusion, this study applied genome-wide screens, novel and established molecular techniques, and multiple murine models of GBS colonization and invasive disease to identify and characterize a GntR-class transcription factor, MrvR, with key roles in multiple virulence-related phenotypes. This newly described transcription factor presents an appealing subject for further mechanistic study and may be a target for novel pharmaceutical approaches to limit GBS virulence through modulation of this molecule's activities.

Methods

Ethics statement

Animal experiments were performed under approved IACUC protocols at NYU (s16-01356) and University of Pittsburgh (20016575). Adult phlebotomy for hemolysis assays was conducted under a University of Pittsburgh approved IRB protocol (19110106). Collection of anonymous, discarded amniotic fluid was conducted under an approved exemption from the NYU IRB.

Statistical analyses

Statistics for Tn-seq were determined with ESSENTIALS software [50] and RNA-seq statistical tests were performed with DESeq 2 [135], using visualization packages in R to generate principal component analysis and heatmap images. Remaining statistics for figures were calculated using Prism for macOS v. 8.4.3 (Graphpad Software, San Diego, CA).

Bacterial strains and growth conditions

GBS strains A909 (serotype Ia, sequence type 7) and CNCTC 10/84 (serotype V, sequence type 26) and their derivatives were grown at 37˚C (or 28˚C when the temperature-sensitive pMBsacB plasmid was present and extrachromosomal) under stationary conditions in tryptic soy (TS) medium (Fisher Scientific cat. # DF0370-17-3), supplemented with 5 μg/ml erythromycin, 150 μg/ml spectinomycin, or rifampin 10 μg/ml as needed for selection. *Escherichia coli* was grown at 37˚C (or 28˚C with extrachromosomal pMBsacB present) with shaking in Luria-Bertani (LB) medium (Fisher Scientific cat. # DF9446-07-5) supplemented with 300 μg/ml erythromycin and 150 μg/ml spectinomycin as needed for selection.

Tn-seq on GBS grown in human amniotic fluid

Discarded, anonymous amniotic fluid from amniocentesis was obtained from the NYU-Langone Medical Center Department of Obstetrics and Gynecology. Samples were stored frozen at -20˚C, then thawed on ice. Before use in outgrowth experiments, the amniotic fluid was passed through a 0.2 μm sterile filter.

A previously described saturated transposon mutant library in an A909 background [41] was thawed from frozen stock. The library was washed twice in sterile PBS to remove glycerol cryoprotectant, then resuspended in 3 mL PBS and seeded into 100 mL of TS broth with erythromycin selection. After overnight outgrowth, 20 mL of the library was seeded into fresh TS broth with erythromycin and allowed to grow to mid-log phase (OD_{600} = 1). 120 mL of this culture was then pelleted and washed twice with PBS, then resuspended in 1 mL of PBS.

50 μL of this concentrated library was then used to seed either 5 mL of amniotic fluid prewarmed to 37˚C or control TS broth. The seeded amniotic fluid and TS was allowed to grow overnight. Unseeded control amniotic fluid samples were also incubated and plated the following morning to ensure that there was no contamination present.

After 16-hour outgrowth, the TS and amniotic fluid samples were transferred into 250 mL aliquots of TS. These were grown overnight, then genomic DNA was purified from 90 mL of each culture using the MoBio Powersoil DNA Extraction Kit (cat. # 128888) according to manufacturer instructions. Purified DNA was subsequently digested with MmeI and used for barcoded terminal adapter ligation, PCR, and sequencing on a 150-nt paired-end run of the Illumina (San Diego, CA, USA) HiSeq 4000 platform, with a target number of reads per library of 50 million and subsequent demultiplexing as previously described [41,42].

We used ESSENTIALS, a publicly available Tn-seq analysis server, to analyze our data [50]. ESSENTIALS generates a plot of genome-wide $\log_2$ fold-change values for actual-versus-expected transposon detection. Bimodality in this plot indicates separate gene populations—those with approximately the expected number of transposon insertions detected in the experimental condition, and those with fewer than expected detected insertions. The latter group represents the set of conditionally essential genes, and the local minimum between the two modal peaks can be used to generate a cutoff value between nonessential and conditionally essential genes. In the case of our amniotic fluid Tn-seq experiment, the local minimum was at a $\log_2$ fold-change value of -3.22. The five candidate genes evaluated had $\log_2$ fold-change values below this cutoff (**S1 Data**).

Development of a GBS CRISPRi system for gene expression knockdown

To generate GBS expressing dCas9, we used the mutagenesis plasmid pMBsacB in GBS strain 10/84 as previously described [88]. Two separate synthetic, double-stranded DNA fragments, 800 to 1000 nt in length, were designed and ordered from Genscript (Piscataway, NJ, USA). The fragments matched the native 10/84 *cas9* coding sequence except for the two missense mutations, D10A and H840A, needed to render the enzyme catalytically inactive. These fragments were cloned into pMBsacB using Gibson assembly and used to transform chemically competent DH5α *E. coli* (New England Biolabs, Ipswich, MA, USA) according to manufacturer instructions. We confirmed proper cloning by Sanger sequencing of miniprepped plasmid DNA, which we then used to transform electrocompetent GBS as previously described [88,136,137]. We performed the C-terminal (H840A) mutagenesis first, following the protocol we have described previously [88]. Once this mutation was generated and confirmed by Sanger sequencing, we made those GBS competent and created the second mutation using identical techniques.

p3015b is a shuttle vector originally derived from pVPL3004 [67]. We used PCR, synthetic DNA, and Gibson assembly approaches to make multiple changes to this plasmid for use in GBS. The kanamycin resistance cassette was changed to the erythromycin resistance gene; the *cas9* gene from *S. pyogenes* was removed; and the tracrRNA sequence downstream of the dual BsaI restriction sites used for protospacer introduction was replaced with a new sequence that conforms to the predicted folding structure of the native GBS tracrRNA sequence (**S1 Fig**). We also sought to introduce anhydrotetracycline inducibility of sgRNA expression by cloning a *tetR* coding sequence and a 2x tetO inducible promoter upstream of the sgRNA coding sequence. Despite extensive efforts, however, we could not suppress baseline sgRNA expression in GBS to the point that gene knockdown was inducible, so the plasmid was used for constitutive sgRNA expression in GBS without anhydrotetracycline addition.

Targeting protospacers were designed using the Broad Institute's online sgRNA design tool [89,90]. Target sequences were selected based on their antisense orientation and, where possible, position in the first half of the coding sequence. Protospacer oligonucleotide sequences were ordered from Integrated DNA Technologies (Coralville, IA, USA) and cloned into BsaI-digested 3015b as originally described by Jiang et al. in their description of pCas9, from which pVPL3004 was developed [138].

qRT-PCR testing for gene silencing

Each of the ten CRISPRi knockdown GBS strains and the non-targeted control strain were grown in TS broth to stationary phase. RNA was purified using the Ribopure Bacteria RNA Purification Kit (Thermo cat. # AM1925), then DNA-depleted with DNase treatment as per kit instructions. The DNase treatment was repeated twice to eliminate any trace

contamination, then cDNA was reverse transcribed using the Applied Biosystems High-Capacity Reverse Transcription Kit (cat. # 4368814). A reverse transcriptase-negative control condition was performed for each sample. qRT-PCR was performed with Bio-Rad SSOAdvanced Universal SYBR Green Supermix (cat. # 1725270) and oligonucleotide primers specific for each of the five targeted genes. The GBS *recA* gene was used as a normalization control. Reactions were performed on a Bio-Rad CFX96 real time PCR thermocycler. After normalization to *recA* expression, each target gene's expression was compared between the knockdown strain and the non-target control strain. This experiment was performed with triplicate samples across two independent replicates.

CRISPRi multiplex competition assay

Cultures of 10/84 dCas9 transformed with p3015b plasmid bearing targeting protospacers against candidate conditionally essential genes were grown overnight in selective broth. A control strain with p3015b plasmid containing a sham protospacer with no matching sequence in the GBS chromosome was grown as a control. The 11 cultures were spun down and washed twice in PBS, then resuspended and normalized to an OD_{600} of 0.8. These suspensions were then plated as serial dilutions to confirm that the starting CFU concentrations were approximately equal.

500 μL from each of the 11 normalized GBS suspensions were then combined to make a starting mixed culture. A sample of this mixed culture was used for plasmid DNA purification using the Thermo MagJET plasmid DNA Kit (cat. # K2791) according to manufacturer instructions.

Amniotic fluid or TS broth containing erythromycin for continued plasmid selection was pre-warmed to 37˚C and seeded 1:50 with the mixed culture, then allowed to grow stationary overnight. 24 hours after seeding, plasmid DNA was extracted from the amniotic fluid and TS samples.

At both the starting and 24-hour timepoints, prior to purification, DNA from dead bacteria was removed using ethidium monoazide using techniques described by Soejima et al. [139]. Ethidium monoazide—which binds to extracellular DNA or DNA within dead bacteria, but not to DNA within live cells—was added to a final concentration of 10 μg/mL, after which the cultures were allowed to incubate at 4˚C for five minutes. They were then placed under a high intensity white light source, which destroys DNA bound to ethidium monoazide. The treated samples were then spun down, washed once in PBS, then used for plasmid purification.

qPCR on purified plasmid samples from the initial and 24-hour timepoints was performed using Applied Biosystems Power SYBR Green Master Mix (Thermo cat. #4368577) on a BioRad (Hercules, CA, USA) CFX384 real-time PCR thermocycler. The different plasmids present were detected using a conserved reverse primer and a forward primer complementary to either one of the targeting protospacer sequences or the sham protospacer sequence. We also used a pair of normalization primers complementary to plasmid sequences distant from the protospacer cloning site. This strategy allowed determination of relative abundances of each of the targeting protospacers (and the sham control) relative to the total plasmid concentration in each sample.

Competition indices for each knockdown strain were calculated using the formula: $\ln((NE^{target}{}_{T24}/NE^{target}{}_{T0})/(NE^{sham}{}_{T24}/NE^{sham}{}_{T0}))$ where NE is normalized expression scaled to total plasmid quantity, target and sham reflect targeting and control plasmids, and T0 and T24 represent samples from the initial mixed culture or from the 24-hour timepoint, respectively. qPCR was performed twice, with two to three technical replicates per primer pair. Competition indices for the knockdown strains were normalized to survival for each strain in TS broth.

Generation of the mrvR knockout and its complemented control strain

A synthetic double-stranded DNA fragment was designed to contain the chloramphenicol acetyltransferase gene surrounded by 500-nt homology arms that match upstream and downstream sequences flanking the *mrvR* open reading frame in 10/84. This mutagenesis cassette was cloned into pMBsacB using Gibson assembly, then used to transform electrocompetent wild type 10/84. Temperature- and sucrose-based selection and counterselection were used to isolate single-cross and double-cross plasmid insertion and excision mutants, which were confirmed using targeted PCR and Sanger sequencing as previously described [88].

To complement the gene deletion, the wild type 10/84 *mrvR* gene and 75 nt of upstream promoter sequence were amplified using PCR and cloned into pBSU101 in place of the *cfb* promoter and green fluorescent protein gene present in the original plasmid [93]. This plasmid was then used to transform the knockout strain, using spectinomycin for positive selection. Photographs and light micrographs of wild type 10/84, the *mrvR* knockout, and the complemented control strain at stationary phase are included in **S4 Fig**.

Amniotic fluid competition assays with CFU quantification

In order to identify wild type and knockout genetic backgrounds following competition in amniotic fluid, we used strains with common antibiotic resistance phenotypes that emerge from isolated missense mutations from single nucleotide polymorphisms. Amniotic fluid or TS broth was seeded with either a) a 10/84 strain with a defined mutation in the *rpoB* gene that confers rifampin resistance [140] and a spontaneous streptomycin-resistant *mrvR* knockout clone or b) the rifampin-resistant 10/84 strain transformed with empty pBSU101 (for spectinomycin resistance) and the complemented, streptomycin-resistant knockout strain. After 24 hours of outgrowth, these mixtures were plated for CFU enumeration on nonselective media, rifampin-containing media, and streptomycin-containing media. This permitted determination of total growth and allowed discrimination between the knockout and wild type strains.

Competition indices were calculated using colony forming unit (CFU) density per mL, where competition index = $\ln((CFU^{expt}{}_{T24}/CFU^{expt}{}_{T0})/ (CFU^{WT}{}_{T24}/CFU^{WT}{}_{T0}))$; here, expt represents the experimental strain (either knockout or control) and WT is wild type 10/84. Assays were performed with three replicates for the knockout and four replicates for the complemented strain. The experiment was repeated twice for each strain; data in **Fig 2** is from a representative replicate.

Hemolysis assays

Whole cell GBS was used in hemolysis assays on washed human erythrocytes as previously described [42]. The assay was performed in triplicate and the experiment was repeated twice. Data in **Fig 2** is from a one of the experimental replicates.

Growth curve analysis

Wild type and *mrvR* knockout GBS were grown to late logarithmic phase in TS broth. The two cultures were then normalized to an OD_{600} of 1.0, then diluted 1:50 in broth. Triplicate samples were then instilled into a clear, flat-bottom 96-well plate, the lid of which had been treated with sterile defogging solution. OD_{600} absorbance readings were taken every 10 minutes, with a brief shaking step before each read, using a Molecular Devices (San Jose, CA, USA) SpectraMax M4 plate reader set to 37˚C. The experiment was repeated twice with triplicate growth wells for each strain; data shown are from one experimental replicate.

Biofilm assays

10 μL of stationary-phase GBS was used to seed 1 mL of fresh broth with appropriate antibiotic selection and 5% glucose supplementation in a 12-well, clear-bottom plate, which was then allowed to grow for 24 hours at 37˚C. Preparations were then photographed and 10 μL of supernatant was used to prepare a Gram stained slide for microscopy following standard protocols (S4 Fig). The plate was rocked gently on an orbital shaker for 1 minute to resuspend non-adherent bacteria, then the media was carefully removed and transferred to a fresh plate. OD_{600} absorbance readings of the planktonic phase bacteria were recorded.

The plate that grew overnight was then used to stain the residual biofilms. 500 μL of 1% crystal violet was carefully added to each well, being cautious not to disturb the biofilm. After 10 minutes of gentle shaking at room temperature, the stain was removed and each well was washed three times in 1 mL of sterile PBS. After the final wash, the stained biofilm was allowed to dry, then solubilized with 1 mL of a 20% acetone/80% ethanol solution. Absorbance at 550 nm was measured. Biofilm indices were calculated as OD_{550}/OD_{600}. The experiment was performed three times with twelve technical replicates for each condition. Data in Fig 2 is from a representative experimental replicate.

Murine vaginal colonization model

Vaginal colonization of nonpregnant C57BL/6J mice was performed as previously described by Randis et al. [13] with minor modifications.

6- to 8-week old mice were injected subcutaneously with 0.5 mg β-estradiol on two successive days to synchronize estrus. On the third day, stationary phase GBS was pelleted and resuspended in a 1:1 mixture of PBS and a sterile 10% gelatin solution to enhance viscosity. The mixtures were diluted and plated for CFU enumeration. Mice were vaginally colonized with 50 μL, corresponding to 10^7 CFU (n = 15 per condition).

Following colonization, mice were single-housed. After 48 hours, an initial swab to detect colonization was performed. A sterile nasopharyngeal swab was moistened in 300 μL sterile PBS, then inserted into the murine vagina and rotated three times, after which it was replaced in the PBS and swirled to release adherent GBS. The PBS was diluted and plated for CFU enumeration on GBS-specific Chromagar plates (Chromagar, Paris, France, cat. # SB282), which were then grown overnight at 37˚C.

Mice with established vaginal colonization, based on the 48-hour swab, were then swabbed three times weekly (Monday, Wednesday, and Friday) following the above protocol. Colonization clearance was defined as two sequential swabs with no detectable GBS.

Chorioamnionitis and preterm delivery model

The murine chorioamnionitis/early-onset sepsis model was performed as previously described [13] with minor modifications. Two- to four-month old BALB/c mice were mated and plug-positive female mice were monitored for pregnancy by physical examination and serial weights.

On pregnancy day 13, mice were vaginally colonized with 10^7 CFU of either wild type 10/84 or the *mrvR* knockout as in the vaginal colonization model (without the preceding estradiol injections). Following colonization, they were single-housed and monitored daily for preterm delivery. If delivery occurred prior to day 17, this outcome was considered chorioamnionitis with preterm birth. Mice that remained pregnant on day 17 were sacrificed and dissected. Each fetus was examined for signs of intrauterine fetal demise (significant pallor or hyperemia, visible skin sloughing or purulence, or evidence of ongoing fetal resorption). An insulin needle

was used to withdraw amniotic fluid from within the fetal membranes, after which placentas and fetuses were isolated and homogenized.

Amniotic fluid and tissue homogenates were diluted and plated on Chromagar plates for CFU enumeration, which was performed after overnight plate growth at 37˚C.

The experiment was continued until 11 mice had been successfully colonized with both strains. Four mice inoculated with wild type GBS did not colonize and three mice inoculated with the knockout strain did not colonize. Pregnancy tissue data from these mice are not included in the analysis.

Generation of luciferase reporter GBS

A toxin-antitoxin stabilized shuttle vector expressing the firefly luciferase gene, pLZ12Km2-P23R:TA:ffluc, was a gift from Thomas Proft (Addgene plasmid # 88900; http://n2t.net/addgene:88900; RRID:Addgene_88900). We used Gibson assembly techniques to excise the kanamycin resistance marker on pLZ12Km2-P23R:TA:Ffluc and replace it with an erythromycin resistance gene. The new plasmid, called pFfluc-Erm, was purified from *E. coli* and used to transform electrocompetent wild type 10/84 and the *mrvR* knockout.

In order to fluoresce, GBS bearing the pFfluc-Erm plasmid must be exposed to the cofactor D-luciferin (Millipore Sigma cat. # L9504), which was prepared in a filter-sterilized stock solution at a concentration of 28 mg/mL in water. We performed *in vitro* imaging of serial dilutions of liquid cultures of GBS transformed with pFfluc-Erm combined 1:1 with D-luciferin stock and determined the level of fluorescence detection at 290,000 CFU/mL.

Adult mouse sepsis model with in vivo imaging

Six- to eight-week old female BALB/c mice were injected intraperitoneally under general anesthesia with 10^8 CFU of PBS-washed, stationary phase WT 10/84 or *mrvR* knockout 10/84 bearing the pFfluc-Erm plasmid and 500 μg of D-luciferin in 500 μL PBS. Immediately after the injection, mice were imaged on a Perkin-Elmer (Waltham, MA, USA) IVIS Lumina Series II imaging instrument with a 1-minute exposure time.

On subsequent days, surviving mice were injected intraperitoneally with 560 μg D-luciferin in sterile water then imaged after 10–15 minutes using a 1-minute exposure time. Mice that cleared their luciferase signal were subsequently observed for five days.

For both strains, 15 mice were injected. Three mice in the knockout condition died within several minutes of intraperitoneal bacterial injection on the first day of the experiment, with evidence of internal hemorrhage. These mice were assumed to have suffered organ injury related to the injection procedure and were not included in the analysis.

Whole-genome RNA-seq transcriptomic analyses

Wild type 10/84 and the *mrvR* knockout 10/84 strain were grown in TS broth overnight. 13-mL overnight culture samples were used for stationary phase RNA extraction. This culture was also used to seed pre-warmed broth, which was then grown to an OD_{600} 0.3–0.6 (early log phase) or 0.9–1.1 (late log phase), at which point RNA extraction was performed.

We used the Ribopure Bacteria RNA Purification Kit (Thermo cat. # AM1925) according to manufacturer specifications with the following exceptions: the initial bead beating step was performed for 20 minutes; the early log bacterial RNA was extracted from an 85-mL starting culture while late log and stationary phases were extracted from 13-mL cultures. RNA samples were then treated with the DNase and DNase inactivation reagents supplied with the kit. Two independent cultures for each strain/growth phase combination were used for RNA purification, sequencing, and analysis.

Sequencing library preparation was conducted with the Illumina TruSeq total RNA kit according to manufacturer instructions. rRNA depletion was performed using the Ribo-Zero Plus rRNA Depletion kit. Next, random primers initiated first and second strand cDNA synthesis. Adenylation of 3' ends was followed by adapter ligation and library amplification with indexing. Sequencing was performed on an Illumina NextSeq500 platform with paired-end 75-nt reads over 150 cycles.

Trimmed and demultiplexed reads were aligned to the 10/84 genome using Bowtie 2 [82]. These alignments were then used for statistical analysis using DESeq 2 [135], which allowed determination of expression fold-change and p values. Gene set enrichment analyses were performed with Genome2D [94].

Confirmation that the 10/84 prophage region was downregulated in the *mrvR* knockout strain was performed in two steps. Initially, PCR of three segments within the prophage region was performed on genomic DNA from separate cultures of wild type and knockout GBS. Gel electrophoresis of these reactions indicated that the entire region remained in the knockout (**S5A Fig**). Next, qRT-PCR on prophage regions 1 and 2 (using primers 1084 Phage qPCR R1 F/R and 1084 Phage qPCR R2 F/R) was performed as described above.

Principal component analysis and generation of the correlation matrix and heatmaps in **S6 Fig** were performed in R.

Supporting information

S1 Data. GBS amniotic fluid conditionally essential gene analysis. Output from ESSENTIALS analysis of eight A909 library aliquots grown in human amniotic fluid. The table is sorted by $\log_2$ fold-change (D), and the five conditionally essential genes described in the main text are highlighted in yellow. The index (column A) allows sorting by gene locus if set from smallest to largest. At the end of the table there is a kernel density plot, generated by the ESSENTIALS bioinformatic package, which shows $\log_2$ fold-change values for experimental-versus-control transposon insertions. The leftmost local minimum on that plot (-3.22) provides a stringent criterion for conditionally essential genes and was used to select the five candidate genes discussed in the main text.
(PDF)

S2 Data. RNA-seq comparing Δ*mrvR* with wild type 10/84 genome-wide gene expression. Output from DESeq 2 analysis of RNA-seq read alignments. Log_2 fold-change and adjusted p values are provided for three growth phases as described in the text.
(PDF)

S1 Table. Oligonucleotides used in this study.
(PDF)

S1 Fig. GBS CRISPRi sequence data. Alignments of GBS and *S. pyogenes* genomic DNA regions encoding CRISPR-Cas complex components (**A-C**). Predicted folding of gRNA complexes (**D**) generated using the mfold server [141]. Sequence of sgRNA complex used to target candidate genes using GBS CRISPRi system (**E**). Sanger sequence showing the two targeted mutations used to generate dCas9 on the 10/84 chromosome (**F**).
(TIF)

S2 Fig. qRT-PCR evaluation of CRISPRi targeted gene expression. Each silenced strain was assessed for normalized expression of the targeted gene relative to a non-targeted control strain. This experiment was performed with triplicate samples across two independent replicates. ($^{*}p<0.05$, **** $p<0.001$, ns = not significant; t test against a single value of 1, error bars

show standard error surrounding the mean).
(TIF)

S3 Fig. Schematic of qPCR-based competition assays between CRISPRi knockdown strains and a non-targeted control strain. Image created with BioRender.com.
(TIF)

S4 Fig. Stationary phase growth of wild type, knockout, and complemented strains. Strains were grown in TS broth (with spectinomycin selection for the complemented control strain) and photographed after overnight growth in a 24-well plate (**top**). Microscopic examination of Gram-stained preparations did not reveal obvious differences in cellular morphology (**bottom**).
(TIF)

S5 Fig. RNA-seq heatmaps. Genome wide correlation matrix with hierarchical clustering (**A**). Top 500 regulated genes across all RNA-seq samples with hierarchical clustering (**B**).
(TIF)

S6 Fig. PCR targeting three regions within the prophage island found to be downregulated in Δ*mrvR*. Three regions within the prophage island spanning gene loci W903_RS03075 through W903_RS03520 were amplified from wild type and *mrvR* knockout GBS genomic DNA. The PCR products from the two strains were the same size when assessed by gel electrophoresis (**A**). The schematic shows the three amplified regions of the chromosome in red (**B**). qPCR validation of RNA-seq data showing decreased expression of RNA from regions 1 and 2 in the *mrvR* knockout compared to wild type (**C**).
(TIF)

S7 Fig. *mrvR* conservation. Gene synteny plot showing orthologs of the GBS *mrvR* gene in 16 other bacterial species. The plot was generated using the Integrated Microbial Genomes & Microbiomes server on the JGI genome portal (https://img.jgi.doe.gov). Genes are color coded by COG functional prediction. COG categories related to nucleotide metabolism present on the diagram are noted (**A**). Conservation of the *mrvR* coding sequence among 138 sequenced GBS genomes aligned through NCBI BLAST (**B**). The top of the panel shows percent conservation at each nucleotide sequence along the coding sequence. Mismatches in individual sequences (gray lines) are highlighted and color-coded for nucleotide identity.
(TIF)

Acknowledgments

We are grateful to the University of Pittsburgh Center for Research Computing, which maintains the HTC cluster used for bioinformatic analysis of RNA-seq data. William MacDonald and Rania Elbakri in the University of Pittsburgh Health Sciences Sequencing Center assisted with next-generation sequencing of RNA-seq samples. Staff at the University of Maryland Genomic Resource Center assisted with sequencing for Tn-seq. Thomas Proft kindly made the plasmid pLZ12Km2-P23R:TA:ffluc available through Addgene. We thank Thomas Diacovo and Jeffrey Weiser, who shared equipment for multiple experiments in this study. We would also like to thank the three anonymous reviewers who provided thoughtful, helpful feedback on our initial manuscript submission.

Author Contributions

Conceptualization: Allison N. Dammann, Adam J. Ratner, Thomas A. Hooven.

Data curation: Allison N. Dammann, Anna B. Chamby, Andrew J. Catomeris, Kyle M. Davidson, Hervé Tettelin, Jordan L. Elder, Thomas A. Hooven.

Formal analysis: Allison N. Dammann, Adam J. Ratner, Thomas A. Hooven.

Funding acquisition: Adam J. Ratner, Thomas A. Hooven.

Investigation: Allison N. Dammann, Anna B. Chamby, Andrew J. Catomeris, Kyle M. Davidson, Kathyayini P. Gopalakrishna, Mary F. Keith, Jordan L. Elder, Adam J. Ratner, Thomas A. Hooven.

Methodology: Allison N. Dammann, Anna B. Chamby, Andrew J. Catomeris, Jan-Peter van Pijkeren, Adam J. Ratner, Thomas A. Hooven.

Resources: Hervé Tettelin, Jan-Peter van Pijkeren, Adam J. Ratner, Thomas A. Hooven.

Visualization: Kyle M. Davidson, Thomas A. Hooven.

Writing – original draft: Thomas A. Hooven.

Writing – review & editing: Allison N. Dammann, Hervé Tettelin, Kathyayini P. Gopalakrishna, Adam J. Ratner, Thomas A. Hooven.

References

1. Heath PT, Jardine LA. Neonatal infections: group B streptococcus. BMJ clinical evidence. 2014; 2014.
2. Johri AK, Paoletti LC, Glaser P, Dua M, Sharma PK, Grandi G, et al. Group B Streptococcus: global incidence and vaccine development. Nat Rev Microbiol. 2006; 4: 932 942. https://doi.org/10.1038/nrmicro1552 PMID: 17088932
3. Sgro M, Shah PS, Campbell D, Tenuta A, Shivananda S, Lee SK, et al. Early-onset neonatal sepsis: rate and organism pattern between 2003 and 2008. J Perinatol. 2011; 31: 794 798. https://doi.org/10.1038/jp.2011.40 PMID: 21527901
4. Berardi A, Rossi C, Lugli L, Creti R, Reggiani MLB, Lanari M, et al. Group B streptococcus late-onset disease: 2003–2010. Pediatrics. 2013; 131: e361 8. https://doi.org/10.1542/peds.2012-1231 PMID: 23296441
5. Regan JA, Kelbanoff MA, Nugent RP. The Epidemiology of Group B Streptococcal Colonization in Pregnancy. Obstetrics & Gynecology. 1991; 77: 604.
6. Bauserman MS, Laughon MM, Hornik CP, Smith PB, Benjamin DK, Clark RH, et al. Group B Streptococcus and Escherichia coli infections in the intensive care nursery in the era of intrapartum antibiotic prophylaxis. Pediatric Infect Dis J. 2013; 32: 208 212. https://doi.org/10.1097/INF.0b013e318275058a PMID: 23011013
7. Madhi SA, Dangor Z, Heath PT, Schrag S, Izu A, Meulen AS, et al. Considerations for a phase-III trial to evaluate a group B Streptococcus polysaccharide-protein conjugate vaccine in pregnant women for the prevention of early- and late-onset invasive disease in young-infants. Vaccine. 2013; 31: D52–D57. https://doi.org/10.1016/j.vaccine.2013.02.029 PMID: 23973347
8. Cools P, Melin P. Group B Streptococcus and perinatal mortality. Res Microbiol. 2017; 168: 793–801. https://doi.org/10.1016/j.resmic.2017.04.002 PMID: 28435137
9. Yadeta TA, Worku A, Egata G, Seyoum B, Marami D, Berhane Y. Maternal group B Streptococcus recto vaginal colonization increases the odds of stillbirth: evidence from Eastern Ethiopia. Bmc Pregnancy Childb. 2018; 18: 410. https://doi.org/10.1186/s12884-018-2044-2 PMID: 30340553
10. Nan C, Dangor Z, Cutland C, Edwards M, Madhi S, Cunnington M. Maternal group B Streptococcus-related stillbirth: a systematic review. Bjog Int J Obstetrics Gynaecol. 2015; 122: 1437–1445. https://doi.org/10.1111/1471-0528.13527 PMID: 26177561
11. Muñoz P, Llancaqueo A, Rodríguez-Créixems M, Peláez T, Martin L, Bouza E. Group B Streptococcus Bacteremia in Nonpregnant Adults. Arch Intern Med. 1997; 157: 213–216. https://doi.org/10.1001/archinte.1997.00440230087011 PMID: 9009979
12. Reingold A, Watt JP. Group B streptococcus infections of soft tissue and bone in California adults, 1995–2012. Epidemiol Infect. 2015; 143: 3343 3350. https://doi.org/10.1017/S0950268815000606 PMID: 26418351

13. Randis TM, Gelber SE, Hooven TA, Abellar RG, Akabas LH, Lewis EL, et al. Group B Streptococcus β-hemolysin/Cytolysin Breaches Maternal-Fetal Barriers to Cause Preterm Birth and Intrauterine Fetal Demise in Vivo. J Infect Dis. 2014; 210: 265 273. https://doi.org/10.1093/infdis/jiu067 PMID: 24474814

14. Vanderhoeven JP, Bierle CJ, Kapur RP, McAdams RM, Beyer RP, Bammler TK, et al. Group B streptococcal infection of the choriodecidua induces dysfunction of the cytokeratin network in amniotic epithelium: a pathway to membrane weakening. Plos Pathog. 2014; 10: e1003920. https://doi.org/10.1371/journal.ppat.1003920 PMID: 24603861

15. Seo HS, Mu R, Kim BJ, Doran KS, Sullam PM. Binding of glycoprotein Srr1 of Streptococcus agalactiae to fibrinogen promotes attachment to brain endothelium and the development of meningitis. Plos Pathog. 2012; 8: e1002947. https://doi.org/10.1371/journal.ppat.1002947 PMID: 23055927

16. Konto-Ghiorghi Y, Mairey E, Mallet A, Duménil G, Caliot E, Trieu-Cuot P, et al. Dual role for pilus in adherence to epithelial cells and biofilm formation in Streptococcus agalactiae. Plos Pathog. 2009; 5: e1000422. https://doi.org/10.1371/journal.ppat.1000422 PMID: 19424490

17. Beckmann C, Waggoner JD, Harris TO, Tamura GS, Rubens CE. Identification of novel adhesins from group B streptococci by use of phage display reveals that C5a peptidase mediates fibronectin binding. Infect Immun. 2002; 70: 2869 2876. https://doi.org/10.1128/iai.70.6.2869-2876.2002 PMID: 12010974

18. Russell-Jones GJ, Gotschlich EC, Blake MS. A Surface-Receptor Specific for Human-Iga on Group-B Streptococci Possessing the Ibc Protein Antigen. The Journal of experimental medicine. 1984; 160: 1467 1475. https://doi.org/10.1084/jem.160.5.1467 PMID: 6387034

19. Jerlström PG, Talay SR, Valentin-Weigand P, Timmis KN, Chhatwal GS. Identification of an immunoglobulin A binding motif located in the beta-antigen of the c protein complex of group B streptococci. Infection and Immunity. 1996; 64: 2787 2793. https://doi.org/10.1128/IAI.64.7.2787-2793.1996 PMID: 8698509

20. Nagano N, Nagano Y, Taguchi F. High Expression of a C Protein β Antigen Gene among Invasive Strains from Certain Clonally Related Groups of Type Ia and Ib Group B Streptococci. Infect Immun. 2002; 70: 4643 4649. https://doi.org/10.1128/iai.70.8.4643-4649.2002 PMID: 12117978

21. Nizet V, Gibson RL, Chi EY, Framson PE, Hulse M, Rubens CE. Group B streptococcal beta-hemolysin expression is associated with injury of lung epithelial cells. Infection and Immunity. 1996; 64: 3818 3826. https://doi.org/10.1128/IAI.64.9.3818-3826.1996 PMID: 8751934

22. Doran KS, Liu GY, Nizet V. Group B streptococcal beta-hemolysin/cytolysin activates neutrophil signaling pathways in brain endothelium and contributes to development of meningitis. J Clin Invest. 2003; 112: 736 744. https://doi.org/10.1172/JCI17335 PMID: 12952922

23. Doran KS, Chang JCW, Benoit VM, Eckmann L, Nizet V. Group B streptococcal beta-hemolysin/cytolysin promotes invasion of human lung epithelial cells and the release of interleukin-8. J Infect Dis. 2002; 185: 196 203. https://doi.org/10.1086/338475 PMID: 11807693

24. Kaplan A, Chung K, Kocak H, Bertolotto C, Uh A, Hobel CJ, et al. Group B streptococcus induces trophoblast death. Microb Pathogenesis. 2008; 45: 231 235. https://doi.org/10.1016/j.micpath.2008.05.003 PMID: 18599257

25. Lupo A, Ruppen C, Hemphill A, Spellerberg B, Sendi P. Phenotypic and molecular characterization of hyperpigmented group B Streptococci. Int J Med Microbiol. 2014; 304: 717 724. https://doi.org/10.1016/j.ijmm.2014.05.003 PMID: 24933304

26. Liu GY, Doran KS, Lawrence T, Turkson N, Puliti M, Tissi L, et al. Sword and shield: linked group B streptococcal beta-hemolysin/cytolysin and carotenoid pigment function to subvert host phagocyte defense. P Natl Acad Sci Usa. 2004; 101: 14491 14496. https://doi.org/10.1073/pnas.0406143101 PMID: 15381763

27. Hensler ME, Liu GY, Sobczak S, Benirschke K, Nizet V, Heldt GP. Virulence role of group B Streptococcus β-hemolysin/cytolysin in a neonatal rabbit model of early-onset pulmonary infection. The Journal of infectious diseases. 2005; 191: 1287 1291. https://doi.org/10.1086/428946 PMID: 15776375

28. Whidbey C, Vornhagen J, Gendrin C, Samson JM, Doering K, Ngo L, et al. A bacterial lipid toxin induces pore formation, pyroptosis, and infection-associated fetal injury and preterm birth. PLoS pathogens. 2014; 1 41.

29. Whidbey C, Harrell MI, Burnside K, Ngo L, Becraft AK, Iyer LM, et al. A hemolytic pigment of Group B Streptococcus allows bacterial penetration of human placenta. J Exp Medicine. 2013; 210: 1265 1281. https://doi.org/10.1084/jem.20122753 PMID: 23712433

30. Whidbey C, Vornhagen J, Gendrin C, Boldenow E, Samson JM, Doering K, et al. A streptococcal lipid toxin induces membrane permeabilization and pyroptosis leading to fetal injury. Embo Mol Med. 2015; 7: 488 505. https://doi.org/10.15252/emmm.201404883 PMID: 25750210

31. Lamy M-C, Zouine M, Fert J, Vergassola M, Couve E, Pellegrini E, et al. CovS/CovR of group B streptococcus: a two-component global regulatory system involved in virulence. Mol Microbiol. 2004; 54: 1250 1268. https://doi.org/10.1111/j.1365-2958.2004.04365.x PMID: 15554966

32. Santi I, Grifantini R, Jiang S-M, Brettoni C, Grandi G, Wessels MR, et al. CsrRS regulates group B Streptococcus virulence gene expression in response to environmental pH: a new perspective on vaccine development. J Bacteriol. 2009; 191: 5387 5397. https://doi.org/10.1128/JB.00370-09 PMID: 19542277

33. Patras KA, Wang N-Y, Fletcher EM, Cavaco CK, Jimenez A, Garg M, et al. Group B Streptococcus CovR regulation modulates host immune signalling pathways to promote vaginal colonization. Cell Microbiol. 2013; 15: 1154 1167. https://doi.org/10.1111/cmi.12105 PMID: 23298320

34. Faralla C, Metruccio MM, Chiara MD, Mu R, Patras KA, Muzzi A, et al. Analysis of Two-Component Systems in Group B Streptococcus Shows That RgfAC and the Novel FspSR Modulate Virulence and Bacterial Fitness. Mbio. 2014; 5: e00870 14. https://doi.org/10.1128/mBio.00870-14 PMID: 24846378

35. Rozhdestvenskaya AS, Totolian AA, Dmitriev AV. Inactivation of DNA-binding response regulator Sak189 abrogates beta-antigen expression and affects virulence of Streptococcus agalactiae. Plos One. 2010; 5: e10212. https://doi.org/10.1371/journal.pone.0010212 PMID: 20419089

36. Lembo A, BinhTran N-T, Jewell KA, Schmidt BZ, Doran KS, Rajagopal L. Serine/threonine phosphatase Stp1 mediates post-transcriptional regulation of hemolysin, autolysis, and virulence of group B Streptococcus. J Biol Chem. 2011; 286: 44197 44210. https://doi.org/10.1074/jbc.M111.313486 PMID: 22081606

37. Quach D, Sorge NM van, Kristian SA, Bryan JD, Shelver DW, Doran KS. The CiaR response regulator in group B Streptococcus promotes intracellular survival and resistance to innate immune defenses. J Bacteriol. 2009; 191: 2023 2032. https://doi.org/10.1128/JB.01216-08 PMID: 19114476

38. Libby EA, Goss LA, Dworkin J. The Eukaryotic-Like Ser/Thr Kinase PrkC Regulates the Essential WalRK Two-Component System in Bacillus subtilis. Plos Genet. 2015; 11: e1005275. https://doi.org/10.1371/journal.pgen.1005275 PMID: 26102633

39. Klinzing DC, Ishmael N, Hotopp JCD, Tettelin H, Shields KR, Madoff LC, et al. The Two-Component Response Regulator LiaR Regulates Cell Wall Stress Responses, Pili Expression and Virulence in Group B Streptococcus. Microbiology+. 2013; 159. https://doi.org/10.1099/mic.0.064444-0 PMID: 23704792

40. Safadi RA, Mereghetti L, Salloum M, Lartigue M-F, Virlogeux-Payant I, Quentin R, et al. Two-component system RgfA/C activates the fbsB gene encoding major fibrinogen-binding protein in highly virulent CC17 clone group B Streptococcus. Plos One. 2011; 6: e14658. https://doi.org/10.1371/journal.pone.0014658 PMID: 21326613

41. Hooven TA, Catomeris AJ, Akabas LH, Randis TM, Maskell DJ, Peters SE, et al. The essential genome of Streptococcus agalactiae. Bmc Genomics. 2016; 17: 406 418. https://doi.org/10.1186/s12864-016-2741-z PMID: 27229469

42. Hooven TA, Catomeris AJ, Bonakdar M, Tallon LJ, Santana-Cruz I, Ott S, et al. The Streptococcus agalactiae stringent response enhances virulence and persistence in human blood. Infect Immun. 2017; 86: e00612–17. https://doi.org/10.1128/IAI.00612-17 PMID: 29109175

43. Opijnen T van, Camilli A. A fine scale phenotype–genotype virulence map of a bacterial pathogen. Genome Res. 2012; 22: 2541–2551. https://doi.org/10.1101/gr.137430.112 PMID: 22826510

44. Opijnen T van, Camilli A. Current Protocols in Microbiology. Current protocols in microbiology. 2010; Chapter 1: 1E.3.1–1E.3.16. https://doi.org/10.1002/9780471729259.mc01e03s19 PMID: 21053251

45. Opijnen T van, Lazinski DW, Camilli A. Genome-Wide Fitness and Genetic Interactions Determined by Tn-seq, a High-Throughput Massively Parallel Sequencing Method for Microorganisms. Curr Protoc Mol Biology Ed Frederick M Ausubel Et Al. 2014; 106: 7.16.1 7.16.24. https://doi.org/10.1002/0471142727.mb0716s106 PMID: 24733243

46. Opijnen T van, Bodi KL, Camilli A. Tn-seq: high-throughput parallel sequencing for fitness and genetic interaction studies in microorganisms. Nat Methods. 2009; 6: 767 772. https://doi.org/10.1038/nmeth.1377 PMID: 19767758

47. Troy EB, Lin T, Gao L, Lazinski DW, Lundt M, Camilli A, et al. Global Tn-seq analysis of carbohydrate utilization and vertebrate infectivity of Borrelia burgdorferi. Mol Microbiol. 2016; 101: 1003 1023. https://doi.org/10.1111/mmi.13437 PMID: 27279039

48. Valentino MD, Foulston L, Sadaka A, Kos VN, Villet RA, Maria JS, et al. Genes contributing to Staphylococcus aureus fitness in abscess- and infection-related ecologies. Mbio. 2014; 5: e01729–14 e01729-14. https://doi.org/10.1128/mBio.01729-14 PMID: 25182329

49. Solaimanpour S, Sarmiento F, Mrázek J. Tn-seq explorer: a tool for analysis of high-throughput sequencing data of transposon mutant libraries. Plos One. 2015; 10: e0126070. https://doi.org/10.1371/journal.pone.0126070 PMID: 25938432

50. Zomer A, Burghout P, Bootsma HJ, Hermans PWM, Hijum SAFT van. ESSENTIALS: software for rapid analysis of high throughput transposon insertion sequencing data. Plos One. 2012; 7: e43012. https://doi.org/10.1371/journal.pone.0043012 PMID: 22900082

51. Pritchard JR, Chao MC, Abel S, Davis BM, Baranowski C, Zhang YJ, et al. ARTIST: high-resolution genome-wide assessment of fitness using transposon-insertion sequencing. Plos Genet. 2014; 10: e1004782. https://doi.org/10.1371/journal.pgen.1004782 PMID: 25375795

52. DeJesus MA, Zhang YJ, Sassetti CM, Rubin EJ, Sacchettini JC, Ioerger TR. Bayesian analysis of gene essentiality based on sequencing of transposon insertion libraries. Bioinformatics. 2013; 29: 695 703. https://doi.org/10.1093/bioinformatics/btt043 PMID: 23361328

53. Charbonneau ARL, Forman OP, Cain AK, Newland G, Robinson C, Boursnell M, et al. Defining the ABC of gene essentiality in streptococci. Bmc Genomics. 2017; 18: 426. https://doi.org/10.1186/s12864-017-3794-3 PMID: 28569133

54. Grosser MR, Paluscio E, Thurlow LR, Dillon MM, Cooper VS, Kawula TH, et al. Genetic requirements for Staphylococcus aureus nitric oxide resistance and virulence. Plos Pathog. 2018; 14: e1006907. https://doi.org/10.1371/journal.ppat.1006907 PMID: 29554137

55. Breton YL, Belew AT, Freiberg JA, Sundar GS, Islam E, Lieberman J, et al. Genome-wide discovery of novel M1T1 group A streptococcal determinants important for fitness and virulence during soft-tissue infection. Wessels MR, editor. Plos Pathog. 2017; 13: e1006584 28. https://doi.org/10.1371/journal.ppat.1006584 PMID: 28832676

56. Skurnik D, Roux D, Aschard H, Cattoir V, Yoder-Himes D, Lory S, et al. A comprehensive analysis of in vitro and in vivo genetic fitness of Pseudomonas aeruginosa using high-throughput sequencing of transposon libraries. Kazmierczak BI, editor. Plos Pathog. 2013; 9: e1003582 16. https://doi.org/10.1371/journal.ppat.1003582 PMID: 24039572

57. Wilde AD, Snyder DJ, Putnam NE, Valentino MD, Hammer ND, Lonergan ZR, et al. Bacterial Hypoxic Responses Revealed as Critical Determinants of the Host-Pathogen Outcome by TnSeq Analysis of Staphylococcus aureus Invasive Infection. Plos Pathog. 2015; 11: e1005341. https://doi.org/10.1371/journal.ppat.1005341 PMID: 26684646

58. Breton YL, Mistry P, Valdes KM, Quigley J, Kumar N, Tettelin H, et al. Genome-wide identification of genes required for fitness of group A Streptococcus in human blood. Infect Immun. 2013; 81: 862 875. https://doi.org/10.1128/IAI.00837-12 PMID: 23297387

59. Burcham LR, Breton YL, Radin JN, Spencer BL, Deng L, Hiron A, et al. Identification of Zinc-Dependent Mechanisms Used by Group B Streptococcus To Overcome Calprotectin-Mediated Stress. Mbio. 2020; 11. https://doi.org/10.1128/mBio.02302-20 PMID: 33173000

60. Goodman AL, Wu M, Gordon JI. Identifying microbial fitness determinants by insertion sequencing using genome-wide transposon mutant libraries. Nat Protoc. 2011; 6: 1969 1980. https://doi.org/10.1038/nprot.2011.417 PMID: 22094732

61. Yang G, Billings G, Hubbard TP, Park JS, Leung KY, Liu Q, et al. Time-Resolved Transposon Insertion Sequencing Reveals Genome-Wide Fitness Dynamics during Infection. Rubin EJ, editor. Mbio. 2017; 8: e01581–17 13. https://doi.org/10.1128/mBio.01581-17 PMID: 28974620

62. Carey AF, Rock JM, Krieger IV, Chase MR, Fernandez-Suarez M, Gagneux S, et al. TnSeq of Mycobacterium tuberculosis clinical isolates reveals strain-specific antibiotic liabilities. Plos Pathog. 2018; 14: e1006939. https://doi.org/10.1371/journal.ppat.1006939 PMID: 29505613

63. Chen JS, Doudna JA. The chemistry of Cas9 and its CRISPR colleagues. Nat Rev Chem. 2017; 1: 0078. https://doi.org/10.1038/s41570-017-0078

64. Jinek M, Chylinski K, Fonfara I, Hauer M, Doudna JA, Charpentier E. A Programmable Dual-RNA–Guided DNA Endonuclease in Adaptive Bacterial Immunity. Science. 2012; 337: 816–821. https://doi.org/10.1126/science.1225829 PMID: 22745249

65. Qi LS, Larson MH, Gilbert LA, Doudna JA, Weissman JS, Arkin AP, et al. Repurposing CRISPR as an RNA-Guided Platform for Sequence-Specific Control of Gene Expression. Cell. 2013; 152: 1173 1183. https://doi.org/10.1016/j.cell.2013.02.022 PMID: 23452860

66. Bikard D, Jiang W, Samai P, Hochschild A, Zhang F, Marraffini LA. Programmable repression and activation of bacterial gene expression using an engineered CRISPR-Cas system. Nucleic Acids Res. 2013; 41: 7429 7437. https://doi.org/10.1093/nar/gkt520 PMID: 23761437

67. Pijkeren J-P van, Britton RA. High efficiency recombineering in lactic acid bacteria. Nucleic Acids Res. 2012; 40: e76 e76. https://doi.org/10.1093/nar/gks147 PMID: 22328729

68. Smith JD, Suresh S, Schlecht U, Wu M, Wagih O, Peltz G, et al. Quantitative CRISPR interference screens in yeast identify chemical-genetic interactions and new rules for guide RNA design. Genome Biol. 2016; 17: 45. https://doi.org/10.1186/s13059-016-0900-9 PMID: 26956608

69. Peters JM, Koo B-M, Patino R, Heussler GE, Hearne CC, Qu J, et al. Enabling genetic analysis of diverse bacteria with Mobile-CRISPRi. Nat Microbiol. 2018; 4: 1 10. https://doi.org/10.1038/s41564-018-0327-z PMID: 30617347

70. Lopez-Sanchez M, Sauvage E, Cunha VD, Clermont D, Hariniaina ER, Gonzalez-Zorn B, et al. The highly dynamic CRISPR1 system of Streptococcus agalactiae controls the diversity of its mobilome. Mol Microbiol. 2012; 85: 1057–1071. https://doi.org/10.1111/j.1365-2958.2012.08172.x PMID: 22834929

71. Ma K, Cao Q, Luo S, Wang Z, Liu G, Lu C, et al. cas9 Enhances Bacterial Virulence by Repressing theregRTranscriptional Regulator in Streptococcus agalactiae. Infect Immun. 2018; 86: e00552–17. https://doi.org/10.1128/IAI.00552-17 PMID: 29229728

72. Spencer BL, Deng L, Patras KA, Burcham ZM, Sanches GF, Nagao PE, et al. Cas9 Contributes to Group B Streptococcal Colonization and Disease. Front Microbiol. 2019; 10: 1930. https://doi.org/10.3389/fmicb.2019.01930 PMID: 31497003

73. Suvorova IA, Korostelev YD, Gelfand MS. GntR Family of Bacterial Transcription Factors and Their DNA Binding Motifs: Structure, Positioning and Co-Evolution. Plos One. 2015; 10: e0132618. https://doi.org/10.1371/journal.pone.0132618 PMID: 26151451

74. Rigali S, Schlicht M, Hoskisson P, Nothaft H, Merzbacher M, Joris B, et al. Extending the classification of bacterial transcription factors beyond the helix–turn–helix motif as an alternative approach to discover new cis / trans relationships. Nucleic Acids Res. 2004; 32: 3418–3426. https://doi.org/10.1093/nar/gkh673 PMID: 15247334

75. Aravind L, Anantharaman V. HutC/FarR-like bacterial transcription factors of the GntR family contain a small molecule-binding domain of the chorismate lyase fold. Fems Microbiol Lett. 2003; 222: 17–23. https://doi.org/10.1016/S0378-1097(03)00242-8 PMID: 12757941

76. Franco IS, Mota LJ, Soares CM, Sá-Nogueira I de. Probing key DNA contacts in AraR-mediated transcriptional repression of the Bacillus subtilis arabinose regulon. Nucleic Acids Res. 2007; 35: 4755–4766. https://doi.org/10.1093/nar/gkm509 PMID: 17617643

77. Jain D. Allosteric control of transcription in GntR family of transcription regulators: A structural overview. Iubmb Life. 2015; 67: 556–563. https://doi.org/10.1002/iub.1401 PMID: 26172911

78. Lord DM, Baran AU, Soo VWC, Wood TK, Peti W, Page R. McbR/YncC: Implications for the Mechanism of Ligand and DNA Binding by a Bacterial GntR Transcriptional Regulator Involved in Biofilm Formation. Biochemistry-us. 2014; 53: 7223–7231. https://doi.org/10.1021/bi500871a PMID: 25376905

79. Morgan RD, Dwinell EA, Bhatia TK, Lang EM, Luyten YA. The MmeI family: type II restriction–modification enzymes that employ single-strand modification for host protection. Nucleic Acids Res. 2009; 37: 5208–5221. https://doi.org/10.1093/nar/gkp534 PMID: 19578066

80. Breton YL, McIver KS. Genetic manipulation of Streptococcus pyogenes (the Group A Streptococcus, GAS). Curr Protoc Microbiol. 2013; 30: Unit 9D.3. https://doi.org/10.1002/9780471729259.mc09d03s30 PMID: 24510894

81. Breton YL, Belew AT, Valdes KM, Islam E, Curry P, Tettelin H, et al. Essential genes in the core genome of the human pathogen Streptococcus pyogenes. Sci Rep-uk. 2015; 5: 9838. https://doi.org/10.1038/srep09838 PMID: 25996237

82. Langmead B, Salzberg SL. Fast gapped-read alignment with Bowtie 2. Nat Methods. 2012; 9: 357 359. https://doi.org/10.1038/nmeth.1923 PMID: 22388286

83. Robinson MD, Oshlack A. A scaling normalization method for differential expression analysis of RNA-seq data. Genome Biol. 2010; 11: R25. https://doi.org/10.1186/gb-2010-11-3-r25 PMID: 20196867

84. Robinson MD, McCarthy DJ, Smyth GK. edgeR: a Bioconductor package for differential expression analysis of digital gene expression data. Bioinformatics. 2010; 26: 139–140. https://doi.org/10.1093/bioinformatics/btp616 PMID: 19910308

85. Jiang F, Taylor DW, Chen JS, Kornfeld JE, Zhou K, Thompson AJ, et al. Structures of a CRISPR-Cas9 R-loop complex primed for DNA cleavage. Science. 2016; 351: 867 871. https://doi.org/10.1126/science.aad8282 PMID: 26841432

86. Sternberg SH, Redding S, Jinek M, Greene EC, Doudna JA. DNA interrogation by the CRISPR RNA-guided endonuclease Cas9. Nature. 2014; 507: 62–67. https://doi.org/10.1038/nature13011 PMID: 24476820

87. Lier C, Baticle E, Horvath P, Haguenoer E, Valentin A-S, Glaser P, et al. Analysis of the type II-A CRISPR-Cas system of Streptococcus agalactiae reveals distinctive features according to genetic lineages. Frontiers Genetics. 2015; 6: 214. https://doi.org/10.3389/fgene.2015.00214 PMID: 26124774

88. Hooven TA, Bonakdar M, Chamby AB, Ratner AJ. A Counterselectable Sucrose Sensitivity Marker Permits Efficient and Flexible Mutagenesis in Streptococcus agalactiae. Appl Environ Microb. 2019; 85. https://doi.org/10.1128/AEM.03009-18 PMID: 30658970

89. Sanson KR, Hanna RE, Hegde M, Donovan KF, Strand C, Sullender ME, et al. Optimized libraries for CRISPR-Cas9 genetic screens with multiple modalities. Nat Commun. 2018; 9: 5416. https://doi.org/10.1038/s41467-018-07901-8 PMID: 30575746

90. Doench JG, Fusi N, Sullender M, Hegde M, Vaimberg EW, Donovan KF, et al. Optimized sgRNA design to maximize activity and minimize off-target effects of CRISPR-Cas9. Nat Biotechnol. 2016; 34: 184 191. https://doi.org/10.1038/nbt.3437 PMID: 26780180

91. Rosa-Fraile M, Dramsi S, Spellerberg B. Group B streptococcal haemolysin and pigment, a tale of twins. Fems Microbiol Rev. 2014; 38: 932 946. https://doi.org/10.1111/1574-6976.12071 PMID: 24617549

92. Florindo C, Ferreira R, Borges V, Spellerberg B, Gomes JP, Borrego MJ. Selection of reference genes for real-time expression studies in Streptococcus agalactiae. J Microbiol Meth. 2012; 90: 220 227. https://doi.org/10.1016/j.mimet.2012.05.011 PMID: 22634000

93. Aymanns S, Mauerer S, Zandbergen G van, Wolz C, Spellerberg B. High-level fluorescence labeling of gram-positive pathogens. Plos One. 2011; 6: e19822. https://doi.org/10.1371/journal.pone.0019822 PMID: 21731607

94. Baerends RJS, Smits WK, Jong A de, Hamoen LW, Kok J, Kuipers OP. Genome2D: a visualization tool for the rapid analysis of bacterial transcriptome data. Genome Biol. 2004; 5: R37. https://doi.org/10.1186/gb-2004-5-5-r37 PMID: 15128451

95. Tazi A, Disson O, Bellais S, Bouaboud A, Dmytruk N, Dramsi S, et al. The surface protein HvgA mediates group B streptococcus hypervirulence and meningeal tropism in neonates. J Exp Medicine. 2010; 207: 2313 2322. https://doi.org/10.1084/jem.20092594 PMID: 20956545

96. Lalioui L, Pellegrini E, Dramsi S, Baptista M, Bourgeois N, Doucet-Populaire F, et al. The SrtA Sortase of Streptococcus agalactiae is required for cell wall anchoring of proteins containing the LPXTG motif, for adhesion to epithelial cells, and for colonization of the mouse intestine. Infect Immun. 2005; 73: 3342 3350. https://doi.org/10.1128/IAI.73.6.3342-3350.2005 PMID: 15908360

97. Dillon HC, Gray E, Pass MA, Gray BM. Anorectal and vaginal carriage of group B streptococci during pregnancy. The Journal of infectious diseases. 1982; 145: 794 799. https://doi.org/10.1093/infdis/145.6.794 PMID: 7045248

98. Sheen TR, Jimenez A, Wang N-Y, Banerjee A, Sorge NM van, Doran KS. Serine-rich repeat proteins and pili promote Streptococcus agalactiae colonization of the vaginal tract. J Bacteriol. 2011; 193: 6834 6842. https://doi.org/10.1128/JB.00094-11 PMID: 21984789

99. Kalimuddin S, Chen SL, Lim CTK, Koh TH, Tan TY, Kam M, et al. 2015 Epidemic of Severe Streptococcus agalactiae Sequence Type 283 Infections in Singapore Associated With the Consumption of Raw Freshwater Fish: A Detailed Analysis of Clinical, Epidemiological, and Bacterial Sequencing Data. Clin Infect Dis. 2017; 64: S145 S152. https://doi.org/10.1093/cid/cix021 PMID: 28475781

100. Puopolo KM, Madoff LC, Eichenwald EC. Early-onset group B streptococcal disease in the era of maternal screening. Pediatrics. 2005; 115: 1240 1246. https://doi.org/10.1542/peds.2004-2275 PMID: 15867030

101. Stoll BJ. Early-Onset Neonatal Sepsis: A Continuing Problem in Need of Novel Prevention Strategies. Pediatrics. 2016; 138: e20163038 e20163038. https://doi.org/10.1542/peds.2016-3038 PMID: 27940736

102. Weston EJ, Pondo T, Lewis MM, Martell-Cleary P, Morin C, Jewell B, et al. The burden of invasive early-onset neonatal sepsis in the United States, 2005–2008. Pediatric Infect Dis J. 2011; 30: 937 941. https://doi.org/10.1097/INF.0b013e318223bad2 PMID: 21654548

103. Pugni L, Pietrasanta C, Acaia B, Merlo D, Ronchi A, Ossola MW, et al. Chorioamnionitis and neonatal outcome in preterm infants: a clinical overview. J Maternal-fetal Neonatal Medicine. 2016; 29: 1525 1529. https://doi.org/10.3109/14767058.2015.1053862 PMID: 26135227

104. Evans HE, Levy E, Glass L. Effect of amniotic fluid on bacterial growth. Obstetrics & Gynecology. 1977; 49: 35 37. PMID: 401535

105. Boldenow E, Jones S, Lieberman RW, Chames MC, Aronoff DM, Xi C, et al. Antimicrobial peptide response to Group B Streptococcus in human extraplacental membranes in culture. Placenta. 2013; 34: 480 485. https://doi.org/10.1016/j.placenta.2013.02.010 PMID: 23562109

106. Soto E, Espinoza J, Nien JK, Kusanovic JP, Erez O, Richani K, et al. Human β-defensin-2: A natural antimicrobial peptide present in amniotic fluid participates in the host response to microbial invasion of the amniotic cavity. J Maternal-fetal Neonatal Medicine. 2009; 20: 15–22. https://doi.org/10.1080/14767050601036212 PMID: 17437194

107. Varrey A, Romero R, Panaitescu B, Miller D, Chaiworapongsa T, Patwardhan M, et al. Human β-defensin-1: A natural antimicrobial peptide present in amniotic fluid that is increased in spontaneous preterm labor with intra-amniotic infection. Am J Reprod Immunol. 2018; 80: e13031. https://doi.org/10.1111/aji.13031 PMID: 30101464

108. Inge E, Talmi YP, Sigler L, Finkelstein Y, Zohar Y. Antibacterial properties of human amniotic membranes. Placenta. 1991; 12: 285–288. https://doi.org/10.1016/0143-4004(91)90010-d PMID: 1754577

109. Galask RP, Snyder IS. Antimicrobial factors in amniotic fluid. Am J Obstet Gynecol. 1970; 106: 59–65. https://doi.org/10.1016/0002-9378(70)90126-2 PMID: 4983127

110. Espinoza J, Chaiworapongsa T, Romero R, Edwin S, Rathnasabapathy C, Gomez R, et al. Antimicrobial peptides in amniotic fluid: defensins, calprotectin and bacterial/permeability-increasing protein in patients with microbial invasion of the amniotic cavity, intra-amniotic inflammation, preterm labor and premature rupture of membranes. J Maternal-fetal Neonatal Medicine. 2009; 13: 2–21. https://doi.org/10.1080/jmf.13.1.2.21 PMID: 12710851

111. ISMAIL MA, SALTI GI, MOAWAD AH. Effect of Amniotic Fluid on Bacterial Recovery and Growth. Obstet Gynecol Surv. 1989; 44: 571–577. https://doi.org/10.1097/00006254-198908000-00001 PMID: 2668811

112. Ford LC, Kasha W, Heins Y, Delange RJ, Wright JD, Alexander G, et al. Identification of β-lysin as a zinc-dependent antibacterial protein in amniotic fluid. J Obstet Gynaecol. 2009; 2: 79–84. https://doi.org/10.3109/01443618109067421

113. Yang Q, Zhang M, Harrington DJ, Black GW, Sutcliffe IC. A proteomic investigation of Streptococcus agalactiae grown under conditions associated with neonatal exposure reveals the upregulation of the putative virulence factor C protein β antigen. Int J Med Microbiol. 2010; 300: 331 337. https://doi.org/10.1016/j.ijmm.2010.01.001 PMID: 20133196

114. Li Z, Wang S, Zhang H, Zhang J, Xi L, Zhang J, et al. Transcriptional regulator GntR of Brucella abortus regulates cytotoxicity, induces the secretion of inflammatory cytokines and affects expression of the type IV secretion system and quorum sensing system in macrophages. World J Microbiol Biotechnology. 2017; 33: 60. https://doi.org/10.1007/s11274-017-2230-9 PMID: 28243986

115. Wassinger A, Zhang L, Tracy E, Munson RS, Kathariou S, Wang HH. Role of a GntR-Family Response Regulator LbrA in Listeria monocytogenes Biofilm Formation. Plos One. 2013; 8: e70448. https://doi.org/10.1371/journal.pone.0070448 PMID: 23894658

116. Yoshida K-I, Fujita Y, Sarai A. Missense Mutations in the Bacillus subtilis gnt Repressor that Diminish Operator Binding Ability. J Mol Biol. 1993; 231: 167–174. https://doi.org/10.1006/jmbi.1993.1270 PMID: 8510140

117. Zhou Y, Nie R, Liu X, Kong J, Wang X, Li J. GntR is involved in the expression of virulence in strain Streptococcus suis P1/7. Fems Microbiol Lett. 2018. https://doi.org/10.1093/femsle/fny091 PMID: 29635445

118. Li Z-Q, Zhang J-L, Xi L, Yang G-L, Wang S-L, Zhang X-G, et al. Deletion of the transcriptional regulator GntR down regulated the expression of Genes Related to Virulence and Conferred Protection against Wild-Type Brucella Challenge in BALB/c Mice. Mol Immunol. 2017; 92: 99–105. https://doi.org/10.1016/j.molimm.2017.10.011 PMID: 29055858

119. Yoshida K, Ohmori H, Miwa Y, Fujita Y. Bacillus subtilis gnt repressor mutants that diminish gluconate-binding ability. J Bacteriol. 1995; 177: 4813–4816. https://doi.org/10.1128/jb.177.16.4813-4816.1995 PMID: 7642511

120. Li Z, Xiang Z, Zeng J, Li Y, Li J. A GntR Family Transcription Factor in Streptococcus mutans Regulates Biofilm Formation and Expression of Multiple Sugar Transporter Genes. Front Microbiol. 2019; 9: 3224. https://doi.org/10.3389/fmicb.2018.03224 PMID: 30692967

121. Nizet V, Ohtake T, Lauth X, Trowbridge J, Rudisill J, Dorschner RA, et al. Innate antimicrobial peptide protects the skin from invasive bacterial infection. Nature. 2001; 414: 454. https://doi.org/10.1038/35106587 PMID: 11719807

122. Rosini R, Margarit I. Biofilm formation by Streptococcus agalactiae: influence of environmental conditions and implicated virulence factors. Front Cell Infect Mi. 2015; 5: 6. https://doi.org/10.3389/fcimb.2015.00006 PMID: 25699242

123. Patterson JL, Girerd PH, Karjane NW, Jefferson KK. Effect of biofilm phenotype on resistance of Gardnerella vaginalis to hydrogen peroxide and lactic acid. Am J Obstet Gynecol. 2007; 197: 170.e1 170.e7. https://doi.org/10.1016/j.ajog.2007.02.027 PMID: 17689638

124. Pandelidis K, McCarthy A, Chesko KL, Viscardi RM. Role of biofilm formation in ureaplasma antibiotic susceptibility and development of bronchopulmonary dysplasia in preterm neonates. Pediatric Infect Dis J. 2013; 32: 394 398. https://doi.org/10.1097/INF.0b013e3182791ae0 PMID: 23114371

125. Doster RS, Sutton J, Rogers LM, Aronoff DM, Gaddy J. Streptococcus agalactiae induces placental macrophages to release extracellular traps loaded with tissue remodeling enzymes via an oxidative-burst-dependent mechanism. Biorxiv. 2018; 440685. https://doi.org/10.1128/mBio.02084-18 PMID: 30459195

126. Sause WE, Balasubramanian D, Irnov I, Copin R, Sullivan MJ, Sommerfield A, et al. The purine biosynthesis regulator PurR moonlights as a virulence regulator in Staphylococcus aureus. Proc National Acad Sci. 2019; 116: 13563–13572. https://doi.org/10.1073/pnas.1904280116 PMID: 31217288

127. Samant S, Lee H, Ghassemi M, Chen J, Cook JL, Mankin AS, et al. Nucleotide Biosynthesis Is Critical for Growth of Bacteria in Human Blood. Plos Pathog. 2008; 4: e37. https://doi.org/10.1371/journal.ppat.0040037 PMID: 18282099

128. Guo Q, Wei Y, Xia B, Jin Y, Liu C, Pan X, et al. Identification of a small molecule that simultaneously suppresses virulence and antibiotic resistance of Pseudomonas aeruginosa. Sci Rep-uk. 2016; 6: 19141. https://doi.org/10.1038/srep19141 PMID: 26751736

129. Rajagopal L, Vo A, Silvestroni A, Rubens CE. Regulation of purine biosynthesis by a eukaryotic-type kinase in Streptococcus agalactiae. Mol Microbiol. 2005; 56: 1329–1346. https://doi.org/10.1111/j.1365-2958.2005.04620.x PMID: 15882424

130. Jendresen CB, Martinussen J, Kilstrup M. The PurR regulon in Lactococcus lactis—transcriptional regulation of the purine nucleotide metabolism and translational machinery. Microbiology+. 2012; 158: 2026 2038. https://doi.org/10.1099/mic.0.059576-0 PMID: 22679106

131. Lancefield RC, McCarty M, Everly WN. Multiple mouse-protective antibodies directed against group B streptococci. Special reference to antibodies effective against protein antigens. J Exp Medicine. 1975; 142: 165–179. https://doi.org/10.1084/jem.142.1.165 PMID: 1097573

132. Wilkinson HW. Analysis of group B streptococcal types associated with disease in human infants and adults. Journal of clinical microbiology. 1978; 7: 176 179. PMID: 344337

133. Rosa-Fraile M, Rodríguez-Granger J, Haidour-Benamin A, Cuerva JM, Sampedro A. Granadaene: proposed structure of the group B Streptococcus polyenic pigment. Appl Environ Microb. 2006; 72: 6367 6370. https://doi.org/10.1128/aem.00756-06 PMID: 16957264

134. Zhu L, Beres SB, Yerramilli P, Pruitt L, Cantu CC, Olsen RJ, et al. Genetic Basis Underlying the Hyperhemolytic Phenotype of Streptococcus agalactiae Strain CNCTC10/84. J Bacteriol. 2020; 202. https://doi.org/10.1128/JB.00504-20 PMID: 32958630

135. Anders S, Huber W. Differential expression analysis for sequence count data. Genome Biol. 2010; 11: R106. https://doi.org/10.1186/gb-2010-11-10-r106 PMID: 20979621

136. Holo H, Nes IF. High-Frequency Transformation, by Electroporation, of Lactococcus-Lactis Subsp Cremoris Grown with Glycine in Osmotically Stabilized Media. Applied and environmental microbiology. 1989; 55: 3119 3123. https://doi.org/10.1128/AEM.55.12.3119-3123.1989 PMID: 16348073

137. Framson PE, Nittayajarn A, Merry J, Youngman P, Rubens CE. New genetic techniques for group B streptococci: high-efficiency transformation, maintenance of temperature-sensitive pWV01 plasmids, and mutagenesis with Tn917. Applied and environmental microbiology. 1997; 63: 3539 3547. https://doi.org/10.1128/AEM.63.9.3539-3547.1997 PMID: 9293004

138. Jiang W, Cox D, Zhang F, Marraffini LA. RNA-guided editing of bacterial genomes using CRISPR-Cas systems. Nat Biotechnol. 2013; 31: 233 239. https://doi.org/10.1038/nbt.2508 PMID: 23360965

139. Soejima T, Iida K, Qin T, Taniai H, Seki M, Yoshida S. Method To Detect Only Live Bacteria during PCR Amplification ▿. J Clin Microbiol. 2008; 46: 2305–2313. https://doi.org/10.1128/JCM.02171-07 PMID: 18448692

140. Martin-Galiano AJ, Campa AG de la. High-Efficiency Generation of Antibiotic-Resistant Strains of Streptococcus pneumoniae by PCR and Transformation. Antimicrob Agents Ch. 2003; 47: 1257 1261. https://doi.org/10.1128/aac.47.4.1257-1261.2003 PMID: 12654655

141. Zuker M. Mfold web server for nucleic acid folding and hybridization prediction. Nucleic Acids Res. 2003; 31: 3406–3415. https://doi.org/10.1093/nar/gkg595 PMID: 12824337